國 立 交 通 大 學
光 電 工 程 研 究 所

碩士論文

非同步諧波鎖模摻鐿光纖雷射之雷射動力學

Laser Dynamics of Asynchronous Harmonic Mode-Locked Yb-Doped Fiber Laser

研 究 生 ： 王聖閔

指導教授: 賴暎杰 教授

中華民國一百年

非同步諧波鎖模摻鐿光纖雷射之雷射動力學

研究生:王聖閔　　教授:賴暎杰　博士

國立交通大學光電工程研究所

摘要

非同步諧波鎖模光纖雷射具有許多的特性，在光通訊、生醫光電或者超快光學等應用之發展上有很好的潛在價值，這些優良特性包括具高超模噪音抑制比，以及可形成超高重複率且超短的脈衝序列。

在此論文之中，我們首次利用偏振疊加波鎖模、相位調變和環形共振腔在摻鐿的雷射系統中成功達到主被動同步諧波鎖模及非同步諧波鎖模，是首次在正色散介質觀察到非同步諧波鎖模的研究工作。其鎖模脈衝重複率為 10 GHz，非同步偏差頻率可達 94 kHz，而雷射系統在非同步諧波鎖模狀態下之超模噪音抑制比達到 60 dB，較同步諧波鎖模狀態增進 40dB。雷射輸出功率達 20 mW，且波長操作在 1050 nm，使得此雷射在包括生醫光電等應用上也有很大的發展潛力。

Laser Dynamics of Asynchronous Harmonic Mode-Locked Yb-Doped Fiber Laser

Student：Sheng-Min Wang **Advisor：Dr. Yinchieh Lai**

Department of Photonics & Institute of Electro-Optical Engineering

College of Electrical and Computer Engineering

National Chiao-Tung University

Abstract

Asynchronous Harmonic Mode-Locked Ytterbium Doped Fiber Lasers have many characteristics which are of great application potentials in the fields of long-distance optical communication, bio-photonics and ultrafast optics. These advantages include higher super-mode suppression ratios and the capability of generating ultrahigh repetition rate and ultra-short pulse trains.

In this thesis, we demonstrate for the first time an asynchronous harmonic mode-locked ytterbium doped fiber laser with the hybrid mode-locking technique. This is the first observation of the asynchronous harmonic mode-locking in a normal dispersion fiber cavity. The deviation frequency of the laser is 94 kHz and the super-mode suppression ratio is around 60 dB at the 10 GHz asynchronous harmonic mode-locked state. The super-mode suppression ratio increases around 40 dB than the ordinary harmonic mode-locked state. The output power is around 20 mW operating at 1050 nm, a useful wavelength in many applications including bio-photonics.

誌謝

碩士班的兩年時間說長不長，說短也不短，這段時間長到讓我接受了太多人的幫忙以及鼓勵，但也短的讓我覺得一切都上軌道時，卻已經到了畢業的時候了。

首先，要感謝我的指導教授賴暎杰老師，賴老師總是在我遇到研究難題的時候耐心且細心地給我一些相當受用的意見，讓我能更有效率且正確的完成實驗，而在與賴老師討論的過程之中，老師的思考方式也讓我更加瞭解了做研究的方法，重新啟發了我對學術研究的的興趣，在未來的日子中我將謹記賴老師的教誨，更加有信心的面對難題。

感謝鞠曉山學長、項維巍學長、林家弘學長、徐桂珠學姊、許宜蓁學姊不管在工作上或者在日常瑣事上的指導，這些寶貴經驗讓我少走了不少冤忘路，更加快速的達成目標。

也要謝謝實驗室夥伴張家豪、呂柏萱、黃柏崴、何姿媛、甘力行、楊良愉、江國豪、讓我在做實驗之餘，也有相當愉快的研究生生活，每一次的歡笑總讓我更有動力面對接下來的挑戰。

最後，最要感謝的是我的家人，讓我在求學階段能夠沒有後顧之憂的繼續升學。

Contents

Chapter 3: Experimental setup and results

Chapter 4: Conclusions

List of Figures and Tables

Chapter 1

Introduction

1.1 Overview

In the 1960's, fiber lasers were made possible by doping the rare-earth ions likeNd^{3+}, Er^{3+}, Tm^{3+} into glass hosts[1.1]. In the1970's, low-loss optical fibers for wide-bandwidth, long-distance optical communication were invented [1.2]. Pools and Mears et al. had used Er^{3+}-doped fibers to produce the first erbium-doped fiber amplifier（EDFA）. The EDFA becomes a fiber laser with proper optical feedback mechanism [1.3] [1.4]. Due to the several advantages such as high output power, high efficiency, less thermal problem and compact size, the mode-locked fiber laser becomes an important light source for many applications including optical communication and bio-photonics.

In recent years, Ytterbium-doped fiber lasers have attracted significant research interest due to the favorable properties of the Yb-doped glass fibers（good conversion efficiency, wide gain bandwidth, and large saturation energy, et al）, which allow generation of short optical pulses with very large pulse energies or peak powers. The advance of ultrafast optics in the last decade has

allowed us to develop lasers with a variety of features such as ultrashort pulse duration, high peak intensity and/or high repetition rate. Ultrashort laser pulse trains with GHz repetition rates will be useful for many applications in research area like optical communications [1.5], photonic switching [1.6], and so on. Passive mode-locked ytterbium fiber lasers can generate short pulses by means of saturable-absorption or additive-pulse mode locking. However, their pulse repetition rates are difficult to be higher than 1 GHz, limited by the cavity length.

One of the possible methods for achieving high repetition rate pulse trains is the harmonic mode-locking technique. Harmonic mode-locking in ytterbium fiber ring lasers can be achieved with nonlinear polarization evolution （NPE） [1.7] （passive mode-locking） or EO modulation （active mode-locking）. Generally, the order of harmonic mode-locking and the super-mode suppression ratio in passive harmonic mode-locked lasers are smaller than active harmonic mode-locked lasers. Thus for the generation of very high repetition rate stable pulse trains, active mode-locking is a very important technique to be considered. By including passive mode-locking mechanisms in an active mode-locked laser, a hybrid mode-locked laser can be built. It has been demonstrated that the

technique of hybrid mode-locking can be a possible solution for directly generating sub-ps pulses at high repetition rates [1.8].

Because of the optical carrier frequency sweeping effects caused by asynchronous phase modulation, the noise will be shifted away. Nevertheless, nonlinear pulses can resist this frequency shift more. Noises are filtered out by the filtering effect while the nonlinear pulses can still exist in the end. By using this effect, we can get a laser with a high repetition rate and low noises.

1.2 Motivation of the research

Femtosecond fiber lasers have a lot of advantages such that they can be used in many applications. First, for instance, the optical fibers cost very little and the components used in optical fiber system are cheaper than bulk optical system. Second, the bandwidth of rare-earth doped fiber laser can support pulses as short as sub-picosecond and the huge saturation level of optical gain allows to generate high energy optical pulses [1.9]. Third, rare-earth doped fibers have high optical pumping efficiency, such that higher output powers are allowed.

For ytterbium-doped fiber lasers, the gain bandwidth can support pulses as

short as 30 fs [1.10] and the optical pumping efficiency can be as high as 80%. High output power, high peak power and excellent power conversion efficiency allow ytterbium-doped fiber lasers to play an important role applications including those in nonlinear optical microscopy. The 1-μm-wavelength light sources can be used in bio-photonics due to the transparent window of organisms. These characteristic can reduce the damages caused by lasers and increase the transparent depth in organisms. Furthermore, if we increase the repetition rate of the light source, it is possible to enhance the sampling rate in spatial domain or time domain and improve the measurement resolution. However, since the laser repetition rate is limited by the length of laser cavity, it difficult to increase the repetition rate by the mechanism of passive mode-locking. On the contrary, active mode-locking can be much easier to operate at high repetition rates, and we can get higher super-mode suppression ratios by asynchronous harmonic mode-locking. So if we can combine ytterbium gain fiber with the mechanism of asynchronous harmonic mode-locking, we should have a laser operating around 1 μm with high repetition rate and higher super-mode suppression ratios. It may become a useful light source for bio-photonics.

1.3 Organization of the thesis

The present thesis is consisted of four chapters. Chapter 1 is an overview of mode-locked fiber lasers and describes the motivation for doing this research. Chapter 2 describes the principles of different mode-locking techniques and the results by theoretical simulation based on the master equation model. Chapter 3 presents our experimental setup and the obtained results. Finally, in Chapter 4, the discussions and analyses of our results are presented with future expectations.

Reference

[1.1] E. Snitzer, “Optical Maser Action of Nd^{3+} in a Barium Crown Glass”, Phys. Rev. Lett. 7, 444 (1961).

[1.2] T. Miya, Y. Terunuma, T. Hosaka, and T. Miyashita, “Ultimate low-loss single-mode fibre at 1.55 um”, Electron. Lett. 15,106-108 (1979).

[1.3] S. B. Poole, D. N. Payne, R. J. Mears, M. E. Fermann, and R. E. Laming, “Fabrication and characterization of low-loss optical fiber containing rare-earth ions”, J. Lightwave Technol. 4, 870 (1986).

[1.4] R. J. Mears, L. Reekie, I. M. Jauncey, and D. N. Payne, “Fiber Laser with 1.54 um radiation wavelength”, Electron. Lett. 27, 1026 (1987).

[1.5] M. Nakazawa, H. Kubota, K. Suzuki, E. Yamada, and A. Sahara, “Ultrahigh-speed long-distance TDM and WDM soliton transmission technologies”, IEEE J. Quantum Electron., 6, 363-396 (2000).

[1.6] D. A. B. Miller, “ Optical interconnects to silicon”, IEEE J. Quantum Electron., 6, 1312-1317(2000).

[1.7] S. Zhou, D. G. Ouzounov, and F. W. Wise, “Passive harmonic mode-locking of a soliton Yb fiber laser at repetition rates to 1.5 GHz”, Opt. Lett., 31, 1041-1043 (2006).

[1.8] W.-W. Hsiang, C.Y. Lin, M.F. Tien, and Y. Lai, “Direct generation of a 10 GHz 816 fs pulse train from an erbium-fiber soliton laser with asynchronous phase modulation”, Opt. Lett., 30, 2943-2945(2005).

[1.9] J. Limpert, A. Liem, H. Zellmer, A. Tünnermann, S. Knoke, and H.Voelckel, “High-average-power millijoule fiber amplifier system”, Conference on Lasers and Electro-optics, Long Beach, CA (2002).

[1.10] J. Limpert, T. Schreiber, T. Clausnitzer, K. Zöllner, H.-J. Fuchs, E.-B. Kley, H. Zellmer, A. Tünnermann, “High-power femtosecond Yb-doped fiber amplifier”, Opt. Express, 10, 14 (2002).

[1.11] N.G.R. Broderick, H.L. Offerhaus, D.J. Richardson, and R.A. Sammut, “Power Scaling in Passively Mode-Locked Large-Mode Area Fiber Lasers”, IEEE Photon. Technol. Lett. 10, 1718 (1998)

Chapter 2

Theories of mode-locked fiber lasers

2.1 Mode-locking

Fiber lasers can be mode-locked passively by different ways, include semiconductor saturable absorbers, polarization additive pulse mode-locking (also called nonlinear polarization rotation) and nonlinear optical loop mirror [2.1]. Passive mode-locked lasers can easily generate sub-picosecond pulses and high peak powers compared with actively mode-locked fiber lasers.

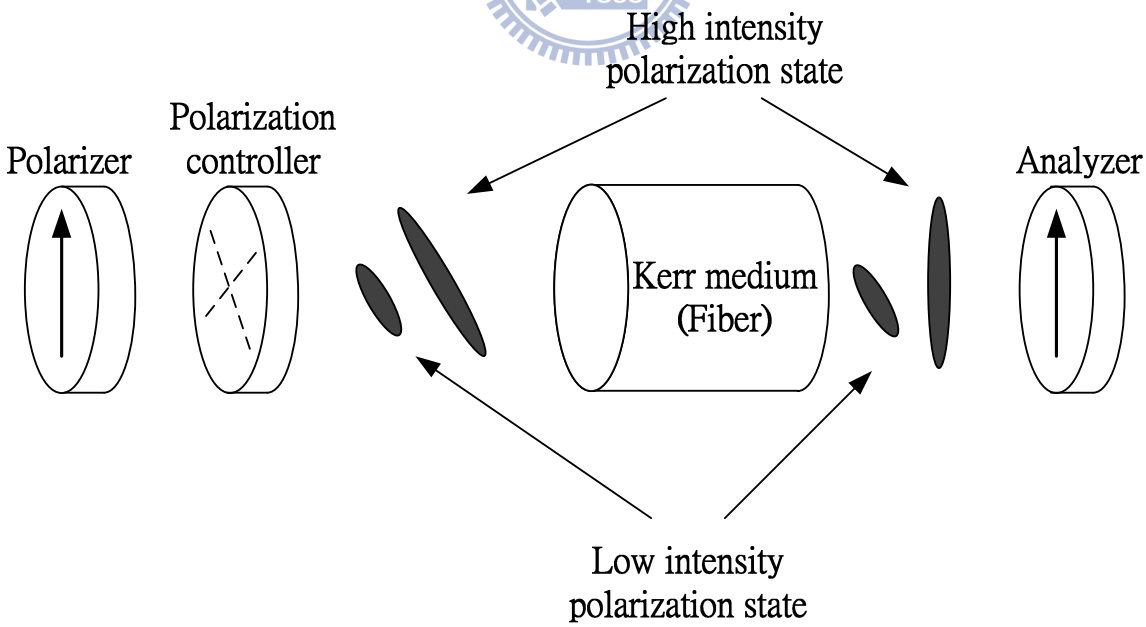

Fig. 2.1 Mechanism of nonlinear polarization rotation

Fiber lasers also can be mode-locked actively by using acousto-optic or electro-optic modulators to produce modulation of amplitude or phase periodically. Mach-Zehnder integrated-optics waveguide-type modulators are typically used for actively mode-locked lasers operated at high frequencies.

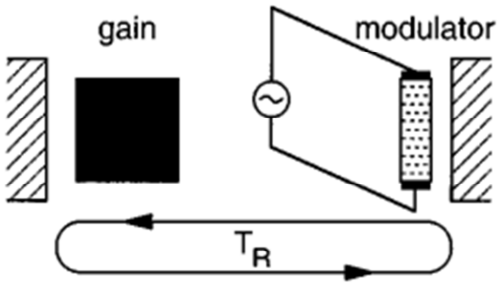

Fig. 2.2 Schematic of an active mode-locked laser [2.2]

In this thesis, our experimental setup is shown in chapter 3 and the setup combines the both mechanisms of passive and active mode-locking.

2.1.1 Active phase modulation mode-locking

Phase modulation mode-locking is a method which modulates the phase of optical field directly to produce short pulses. By modulating the phase of optical field periodically, it can achieve mode-locking without changing the amplitude of optical field. This mechanism can be analyzed both in the frequency domain and in the time domain [2.2].

In the frequency domain, when one longitudinal mode passes through the phase modulator, the modulated signal can be written as,

$$E(t) = E_0 \cos(\omega_0 t + \Delta_m \cos \omega_m)$$

Where Δ_m is the modulation index,

ω_0 is the angular frequency of the longitudinal mode,

Ω_m is the modulation frequency.

It can be expanded as:

$$E(t) = E_0 \sum_{-\infty}^{\infty} J_n(\Delta_m) \cos(\omega_0 t + n\Omega_m t)$$

where J_n is the n-th order Bessel function. Unlimited number of sidebands ($n\Omega_m$) will be generated after phase modulation. These sidebands will combine together to form a periodically pulse train in the time domain if the phases of these modes are locked.

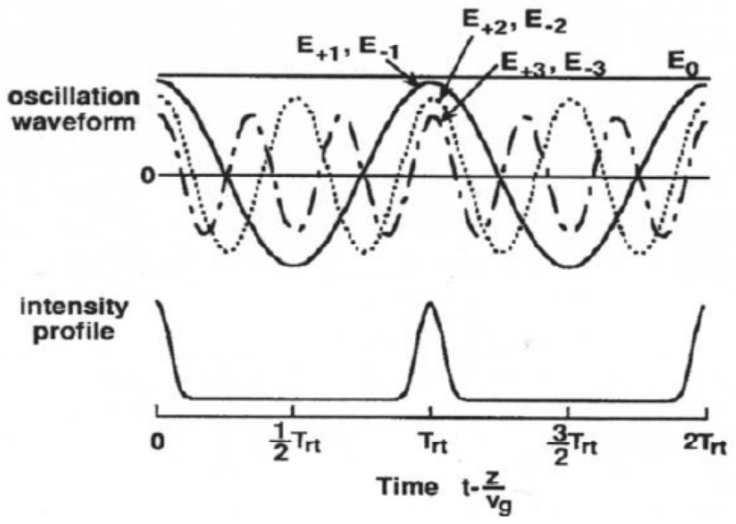

Fig. 2.3 Formulation of pulse train in the time domain

In the time domain, the phase modulator provides a phase change for the optical pulse. Assume the pulsewidth is much smaller than the modulation period, than the Taylor expansion of the optical phase changed by the phase modulator can be expressed as,

$$\varphi(t) = \varphi_0 + \frac{d\varphi}{dt}t + \frac{d^2\varphi}{dt^2}t^2 + \frac{d^3\varphi}{dt^3}t^3 + \cdots$$

where φ_0 is only a constant phase that has no effect on optical pulses.

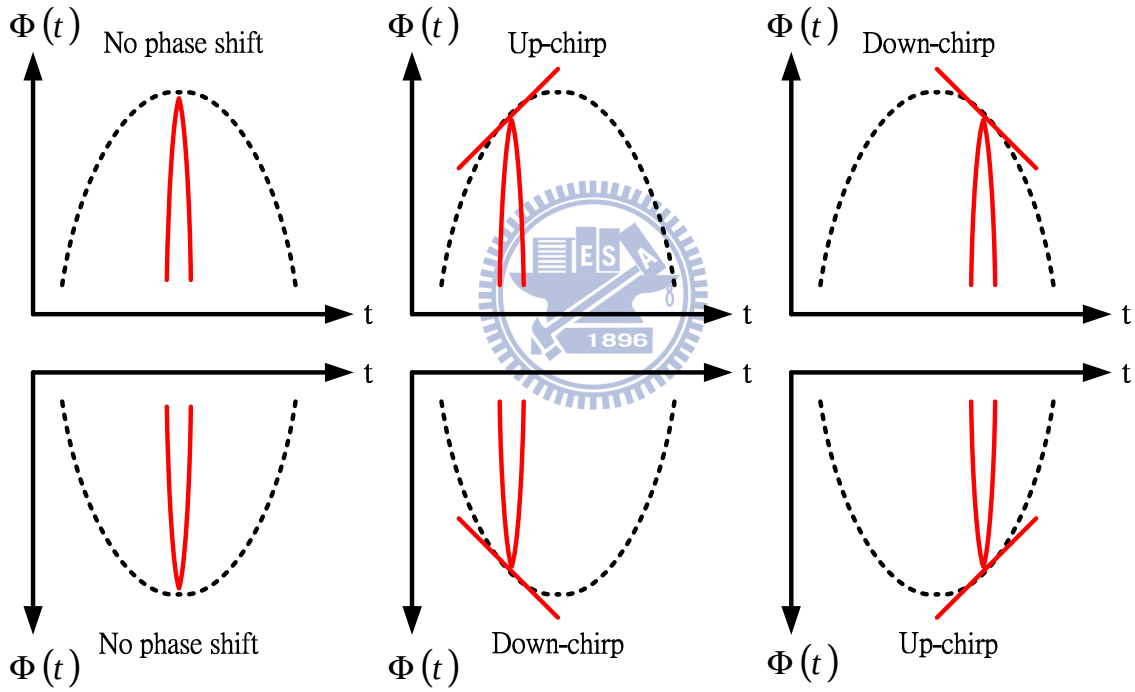

Fig. 2.4 Sketch of phase modulation mode-locking in the time domain

If $\frac{d\varphi}{dt} \neq 0$, the phase modulator will provide a frequency shift of the optical pulse. At next roundtrip, the central frequency of the optical pulse will be shifted again. This process will continue until the central frequency of the optical pulse

is shifted out of the bandwidth of gain media and disappears. Therefore, the pulse only can survive when $\frac{d\varphi}{dt} = 0$, because the central frequency of the optical pulse experiences no change after passing through the phase modulator. For this case, optical pulses will grow in the cavity and form a periodic pulse train.

In fact, from the Fig. 2.4 it can be obviously observed that there are two solution states exist. In most situations, however, only one solution state is stable in the laser cavity because the second order term $\frac{d^2\varphi}{dt^2}$ provides a chirp to the optical pulse. Which solution state can exist in the cavity depends on the group velocity dispersion of intracavity.

2.2 Harmonic mode-locking

Long cavity length can reduce the fundamental frequency of the laser because the fundamental frequency is in inverse proportion to the cavity length. For fiber lasers, the cavity length usually is tens of meters or hundreds of meters such that fundamental frequency can only reach several MHz. Harmonic mode-locking is a method to increase the pulse repetition rate up to the order of GHz or higher.

By increasing the modulation frequency （f_m） which is equal to the integer multiple of the fundamental frequency （Nf_0）. Assume the original electric field can be written as,

$$E(t) = \cos 2\pi\upsilon_0 t$$

the fundamental frequency of the cavity can be written as,

$$f_0 = C/n_{eff}L$$

where n_{eff} is the effective refract index,

and L is the laser cavity length.

The electric field after modulation can be written as,

$$E(t) = (1 + \Delta_m \cos 2\pi N f_0 t)E_0 \cos 2\pi\upsilon_0 t$$

$$= E_0 \cos 2\pi\upsilon_0 t + \Delta_m E_0 \cos \Omega_m t \cos 2\pi\upsilon_0 t$$

$$= E_0 \cos 2\pi\upsilon_0 t + \frac{1}{2}\Delta_m E_0(\cos 2\pi(\upsilon_0 + Nf_0)\, t + \frac{1}{2}\Delta_m \cos 2\pi(\upsilon_0 - Nf_0)t)$$

Here υ_0 is the central frequency of the gain curve, and

Δ_m is the modulation index.

At the harmonic mode-locking state, the υ_0 component will couple with the sidebands separated by Nf_0 and will form N pairs of super-modes. If one observes a super-mode, there are N independent pulses that are separated by

T_R/N in the time domain. In this way, the repetition rate increase to Nf_0.

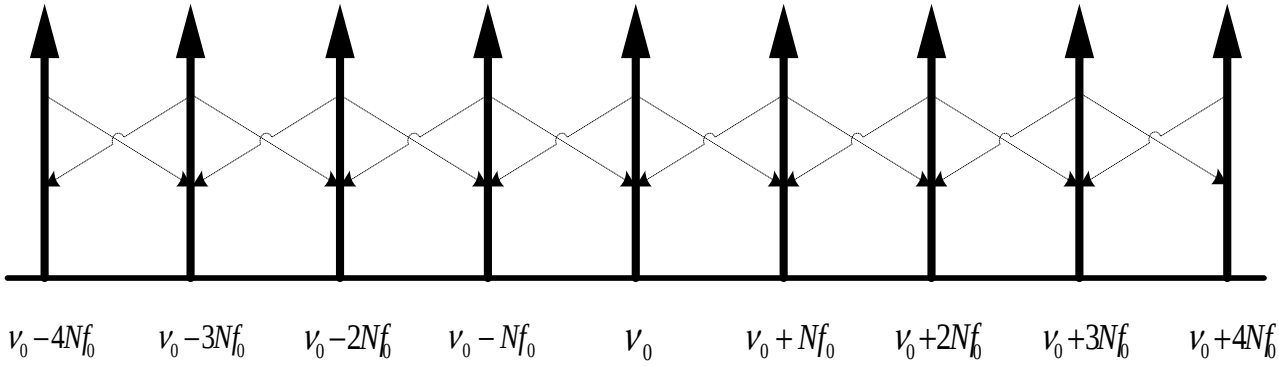

Fig. 2.5 Sketch of the amplitude modulation mode-locking in the frequency domain

Although harmonic mode-locking can increase the repetition rate of optical pulse, the output pulse train may not be stable because the N pair of super-modes in the laser cavity will compete against others. Gain competition can cause power fluctuations or super-mode noises.

2.3 Asynchronous harmonic mode-locking

The studied fiber laser includes the gain, optical band-pass filtering, group velocity （GVD）, self-phase modulation （SPM） and the phase modulation. In active harmonic mode-locked laser, the optical modulator in the laser cavity is driven synchronously. In other word, the modulation frequency is exactly equal to the cavity harmonic frequency.

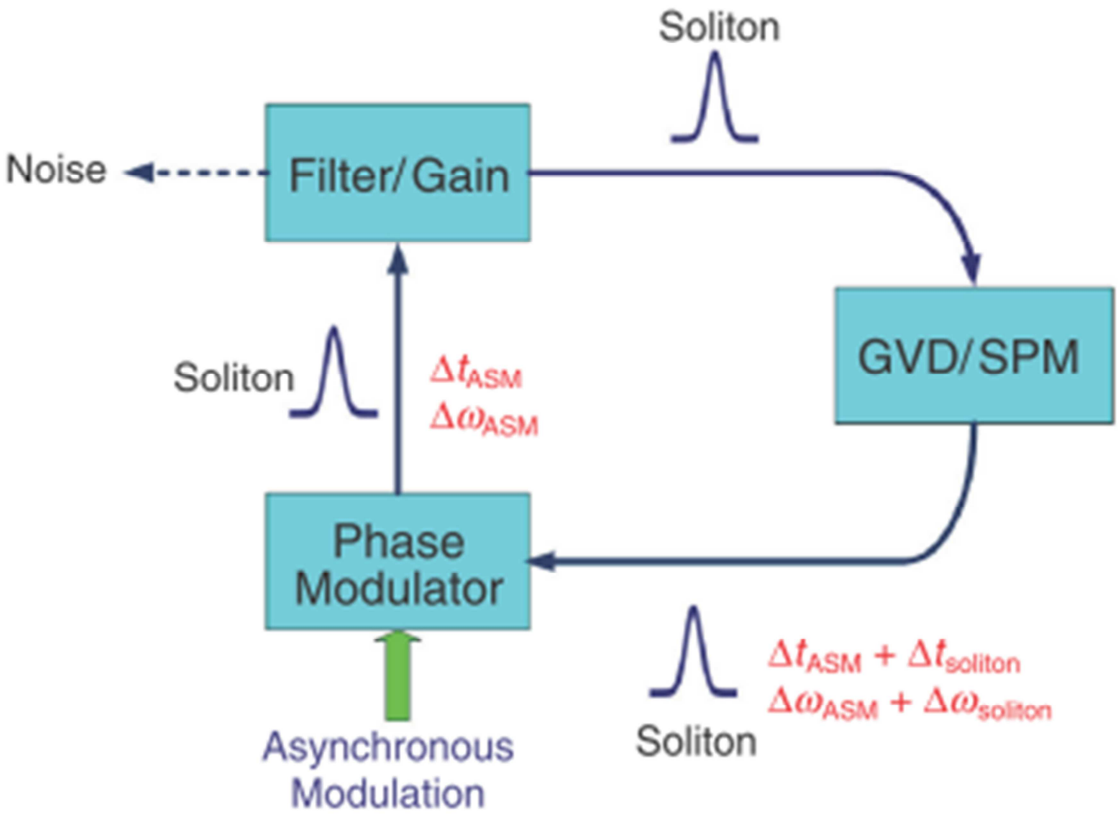

Fig. 2.6 Laser cavity with the gain, filter, GVD, SPM and the phase modulation driven asynchronously

However, in the asynchronous mode-locked lasers [2.3], the modulation frequency and the cavity harmonic frequency have a small deviation frequency from several kHz to tens kHz [2.4]. Since to the modulation signal is driven asynchronously, the optical pulses do not always pass through at the peaks of the modulation signal. For linear optical pulses, they will follow the asynchronous phase modulation signal, and experience large central frequency shifts. Because of the limitation of optical filter and the bandwidth of gain media, the linear pulses will experience huge losses and can not exist in the laser cavity. Nevertheless, optical pulses with nonlinear effects can resist the frequency displacement induced by asynchronous phase modulation and achieve the stable mode-locking state [2.5].

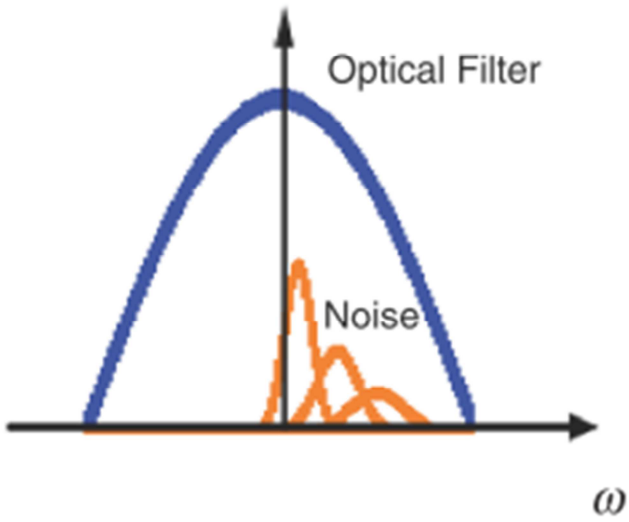

Fig. 2.7 The noise-cleanup effect in the asynchronous soliton mode-locked laser

The mechanism explained above is similar to the effects of the sliding-frequency guiding filter [2.6] in the soliton communication systems. The central frequency of solitons will shift with the variation of the center frequency of the filters in the fiber link during propagation, but the center frequency of the linear noise keeps fixed and will be filtered out by the sliding filters. It provides another advantage for asynchronous mode-locking: a higher SMSR can be obtained, even when here is no explicit intracavity optical devices to suppress the super-mode noises.

In the time domain, the behavior of the pulse train operating at asynchronous active mode-locking is not the same with the synchronous active mode-locking. If the laser is operating at the asynchronous active mode-locking, the pulse train will not only have linear timing walk-off but also periodical timing oscillation.

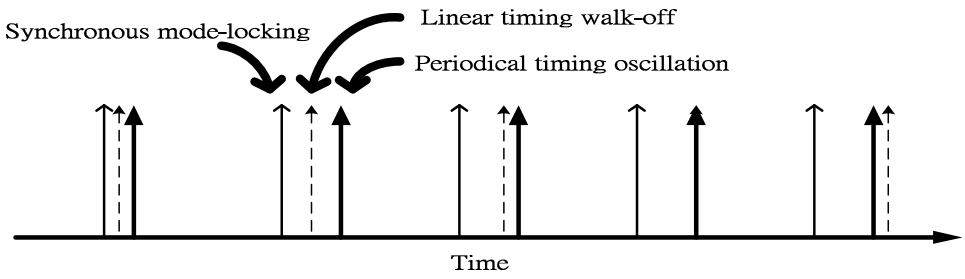

Fig. 2.8 Slow periodic pulse timing oscillation of asynchronous harmonic mode-locking

2.4 Parabolic pulse in Normal dispersion regime

Group velocity dispersion (GVD) within the laser cavity can be the anomalous dispersion or normal dispersion decided by the fiber media and wavelength. For the different net cavity dispersion, there are different operating regimes [2.7].The net group velocity dispersion of the cavity can be normal or anomalous [2.8].

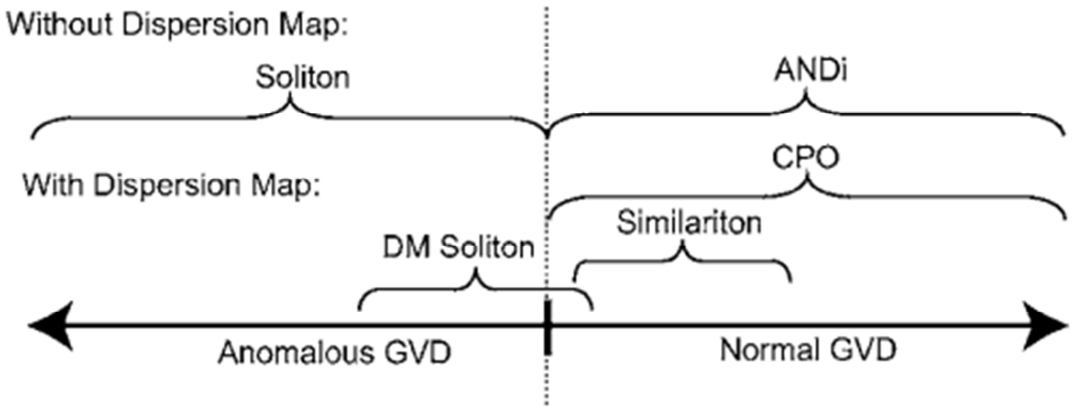

Fig. 2.9 Laser operating regimes according to the net cavity dispersion and the existence of a dispersion map [2.8].

For large net anomalous group velocity dispersion, the nonlinear pulse such as a soliton can be generated due to the balance of nonlinearity (Kerr effect, etc.) and anomalous dispersion [2.9].The fundamental soliton can be stable at only one particular power level pulse energy. If operating at higher power levels, the soliton will evolve into the high order soliton, which is sensitive to perturbations

and will break-up through soliton fission [2.10]. When the net group velocity dispersion approaches zero, the laser operated at the stretched-pulse state. Pulses of the stretched-pulse lasers will breathe (dispersion-managed solitons). The too-large phase shift caused by nonlinear effects generally limits the pulse energy and peak power in the laser cavity. For large net normal group velocity dispersion, the mode-locked laser is expected to produce stable high-energy pulses [2.11]. The shape of the laser pulse is based on spectral filtering of the chirped pulse, which cuts off the temporal wings of the pulse.

For high-power pulse propagation in the normal-dispersion regime, the pulse can avoid from the optical wave breaking. In fact, if the pulse intensity shape is parabolic with a linear frequency chirp, the pulse breaking can be kept off [2.12]. Moreover, if the ultrashort parabolic pulses propagate in a normal-dispersion amplifier, the pulse intensity profile will maintain, and the pulse energy also increase when passing through the gain medium.

We know that a mode-locked fiber laser can be described by the master equation as follows [2.13]:

$$i\frac{\partial \psi(z,T)}{\partial z} = \frac{\beta_2}{2}\frac{\partial^2 \psi(z,T)}{\partial T^2} - \gamma|\psi(z,T)|^2\psi(z,T) + i\frac{g}{2}\psi(z,T)$$

where $\psi(z,T)$ is the slowly varying pulse envelope,

β_2 is the fiber dispersion coefficient,

γ is the fiber Kerr nonlinear coefficient,

g is the amplifier distributed gain coefficient.

The optical field can be written as,

$$\psi(z,T) = A(z,T)e^{i\Phi(z,T)}$$

then the analytic expression for the amplitude $A(z,T)$ and phase $\Phi(z,T)$ of the asymptotic solution ($|T| \le T_p(z)$) can be written as,

$$A(z,T) = A_0 e^{\frac{gz}{3}\sqrt{1-\frac{T^2}{T_p^2(z)}}}$$

$$\Phi(z,T) = \varphi_0 + \frac{3\gamma A_0^2}{2g}e^{\frac{2gz}{3}} - \frac{g}{6\beta_2}T^2$$

$$A_0 = \frac{1}{2}\left(\frac{gU_{in}}{\sqrt{\gamma\beta_2/2}}\right)^{1/3}$$

$$T_p(z) = \frac{6\sqrt{\gamma\beta_2/2}}{g}A_0 e^{\frac{gz}{3}}$$

where U_{in} is the input pulse energy,

A_0 is the parabolic-pulse amplitude,

T_p is the parabolic pulsewidth,

φ_0 is an arbitrary constant.

Then the analytic expression for the amplitude $A_w(z,T)$ and phase $\Phi_w(z,T)$

of the asymptotic solution ($|T| \geq T_p(z)$) can be written as,

$$\psi(z,T) = A_w(z,T)e^{i\Phi_w(z,T)}$$

$$A_w(z,T) = \frac{A_{w0}}{\sqrt{z}} e^{\frac{gz}{2}} e^{-\Lambda\frac{|T|}{z}}$$

$$\Phi_w(z,T) = \Phi_{w0} + \frac{\beta_2 \Lambda^2}{2z} - \frac{T^2}{2\beta_2 z}$$

where A_{w0} and $\Lambda$are determined numerically for particular initial conditions, φ_{w0} is arbitrary constant.

The frequency chirp of pulse envelope can be written as,

$$\Omega(z,T) = -\frac{d\Phi(z,T)}{dT}$$

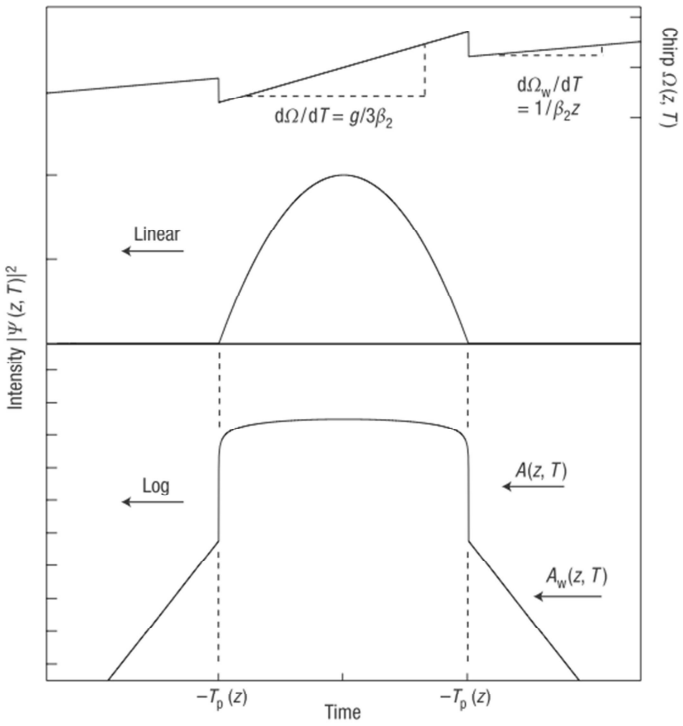

Fig. 2.10 Property of general similariton. Top: parabolic intensity profile （left axis) and linear chirp（right axis）. Bottom: the intensity profile on a logarithmic scale [2.13].

At the central of the pulse, the intensity profile is parabolic and has the linear frequency chirp. Moreover, we can obviously observe that the frequency chirp is independent of propagation distance at the central of the pulse and the frequency chirp can be written as,

$$\Omega(z,T) = \frac{g}{3\beta_2}T$$

The chirp property of propagation distance independence is a good characteristic for optical compressor, because we can easily design the pulse compression system to eliminate the linear chirp of the pulse.

Another characteristic of similariton is that the evolvement of the pulse is different from the soliton pulse when propagation in an amplifier. Soliton can only by stable at a particular power level, or it will become higher order solitons with higher power levels. However, when propagating in the gain medium, the amplitude and pulsewidth of the similariton will increase without changing the intensity temporal profile of the pulse. This distinguishing feature allows similariton be amplified easier than the soliton [2.14].

2.5 Simulation

In general, the mode-locked laser dynamics can be described by a master equation when the pulse round trip change is small. The master equation of asynchronously mode-locked fiber laser can be described as follows [2.11] [2.15]:

$$\frac{\partial u(T,t)}{\partial T} = \left(\frac{g_0}{1+\frac{\int |u|^2 dt}{E_s}} - l_0\right)u + (d_r + jd_i)\frac{\partial^2 u}{\partial t^2} + (k_r + jk_i)|u|^2 u + jM\cos[\omega_m(t+RT)]u$$

Here $u(T,t)$ is the complex field envelope of the pulse,

g_0 is the unsaturated gain, $E_s$is the gain saturation energy,

l_0 is the linear loss,

d_r represents the effect of the optical filtering,

d_i is group velocity dispersion,

k_r modelocking (P-APM),

k_i is the self-phase modulation coefficient,

M is the phase modulation strength,

ω_m is the angular modulation frequency,

t is the time axis measured in the moving frame propagating at a specific

group velocity along with the pulse,

T is the number of the cavity round trip,

R is the linear timing walk-off per roundtrip due to asynchronous phase modulation, which can be expressed by [2.16]:

$$R = N\left(\frac{1}{Nf_R} - \frac{1}{f_m}\right) = \frac{\delta f}{f_R f_m}$$

Here δf is the deviation frequency between the N-th cavity harmonic frequency Nf_R and the modulation frequency f_m.

We have solved the master equation by the method of finite difference. The asynchronous harmonic mode-locked laser parameters are determined based on our past experiences and the parabolic pulses are used as the initial conditions. The evolution of the propagated pulse is shown in Fig. 2.11. From Fig. 2.11, it is clear that a steady state solution has been found and the pulse timing position variation due to asynchronous mode-locking can also be clearly seen.

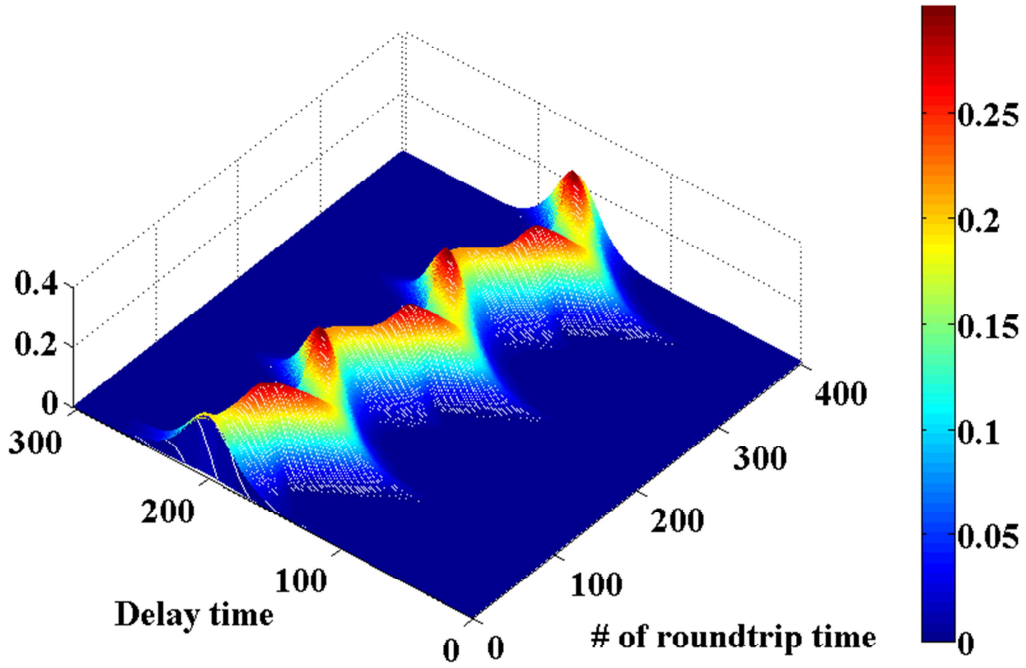

Fig. 2.11 Evolution of pulse intensity profile

We can observe from the above figures that the pulse exhibits the slow periodic variation at the deviation frequency as shown in Fig. 2.11.

Reference

[2.1] L.E. Nelson, D.J. Jones, K. Tamura, H.A. Haus, E.P. Ippen, “Ultrashort-pulse fiber ring lasers”, Appl. Phys. B 65, 277–294 (1997).

[2.2] H. A. Haus, “Mode-locking of lasers,” IEEE J. Sel. Top. Quantum Electron., 6, 1173–1185 (2000).

[2.3] C. R. Doerr, H. A. Haus, and E. P. Ippen, “Asynchronous soliton mode locking”, Opt. Lett. 19, 1958-1960 (1994)..

[2.4] H. A. Haus, D. J. Jones, E. P. Ippen, and W.S. Wong, “Theory of soliton stability in asynchronous modelocking”, IEEE J. Lightwave Technol., 14, 622-627 (1996).

[2.5] W.-W Hsiang, C.-Y Lin, M.-F Tien, and Y. Lai, “Direct generation of a 10 GHz 816 fs pulse train from anerbium-fiber soliton laser with synchronous phase modulation”, Opt. Lett. 30, 2493-2495 (2005).

[2.6] L. F. Mollenauer, J. P. Gordon, and S. G. Evangelides, ‘‘The sliding frequency guiding filter: an improved form of soliton jitter control’’, Opt. Lett. 17, 1575 (1992).

[2.7] A. Chong, W. H. Renninger, and F. W. Wise, “All-normal-dispersion femtosecond fiber laser with pulse energy above 20 nJ”, Opt. Lett. 18, (2007).

[2.8] A. Chong, W. H. Renninger, and F. W. Wise, “Properties of normal-dispersion femtosecond fiber laser”, J. Opt. Soc. Am. B, 25 (2008).

[2.9] Y. Kodama, & A. Hasegawa, “Nonlinear pulse propagation in a monomode dielectric guide”, IEEE J. Quant. Electron., 23, 510–524 (1987).

[2.10] K. Tamura, J. Jacobson, H. A. Haus, E. P. Ippen, and J. G. Fujimoto, “77-fs pulse generation from a stretched-pulse mode-locked all-fiber ring laser”, Opt. Lett., 18, 1080–1082 (1993).

[2.11] H. A. Haus, J. G. Fujimoto, and E. P. Ippen, “Structures for additive pulse mode locking”, J. Opt. Soc. Am. B, 8, 2068–2076 (1991).

[2.12] D. Anderson, M. Desaix, M. Karlson, M. Lisak, & M.L. Quiroga-Teixeiro, “Wave-breaking-free pulses in nonlinear optical fibers”, J. Opt. Soc. Am. B, 10, 1185–1190 (1993).

[2.13] J. M. Dudley, C. Finot, D. J. Richardson and G. Millot, “Self-similarity in ultrafast nonlinear optics”, Nature, 3, 597-603 (2007).

[2.14] V. I. Kruglov, A. C. Peacock, and J. D. Harvey, “Self-similar propagation of parabolic pulses in normal-dispersion fiber amplifiers”, J. Opt. Soc. Am. B, 19, 461 (2002).

[2.15] H. A. Haus, D. J. Jones, E. P. Ippen and W. S. Wong, “Theory of soliton stability in asynchronous mode locking”, J. Lightw. Technol., 14, 622 (1996).

[2.16] W.-W. Hsiang, H.-C. C., Y. Lai, “Laser Dynamics of a 10 GHz 0.55 ps Asynchronously Harmonic Mode locked Er-Fiber Soliton Laser”, IEEE J. Quantum Elect., 46(3), 292. (2010).

[2.17] M. Becker et al., “Harmonic mode locking of the Nd:YAG laser”, IEEE J. Quantum Electron. 8 (8), 687, (1972).

[2.18] N. Onodera, “Supermode beat suppression in harmonically mode-locked erbium-doped fiber ring lasers with composite cavity structure,” Electron.Lett., vol. 33, pp. 962–963, (1997).

[2.19] M. C. Chan, “Hybrid Mode-locking Er-doped Fiber Laser,” Institute of Electro-Optical engineering in National Chiao-Tung University, master thesis (2002).

[2.20] G. T. Harvey and L. F. Mollenauer, “Harmonically mode-locked fiber ring laser with an internal Fabry-Perot stabilizer for soliton transmission,” Opt. Lett. 18, 107 (1993).

[2.21] D. J. Jones, H. A. Haus, and E. P. Ippen, “Subpicosecond solitons in an actively mode-locked fiber laser,” Opt. Lett. 21, 1818 (1993).

[2.22] F. X. Kärtner, D. Kopf, and U. Keller, “Solitary-pulse stabilizationand shortening in actively mode-locked laser,” Opt. Soc. Am. B 12, 486 (1995).

[2.23] D. J. KUIZENGA, and A .E. SIEGMAN “FM and AM mode locking of the homogeneous laser,” IEEE J. Quantum Electron. 6, 694 (1970).

[2.24] W. H. Renninger, A. Chong, and F. W. Wise, “Dissipative solitons in normal-dispersion fiber lasers,” Phys. Rev. A, 77, 023814 (2008).

[2.25] F. Ö. Ilday, J. R. Buckley, W. G. Clark, F.W. Wise, “Self-Similar Evolution of Parabolic Pulses in a Laser,” Phys. Rev. Lett., 92, 21 (2004).

[2.26] M. E. Fermann, V. I. Kruglov, B. C. Thomsen, J. M. Dudley, and J. D. Harvey, “Self-Similar Propagation and Amplification of Parabolic Pulses in Optical Fibers,” Phys. Rev. Lett., 84, 26 (2000).

[2.27] B. Oktem, C. Ülgüdür, and F. Ö. Ilday, “Soliton–similariton fibre laser,” Nature, 4, 307-311 (2010).

Chapter 3

Experimental setup and results

3.1 Experimental setup

The schematic setup of our asynchronous harmonic mode-locked ytterbium doped fiber laser with the ring cavity is shown in Fig. 3.1.

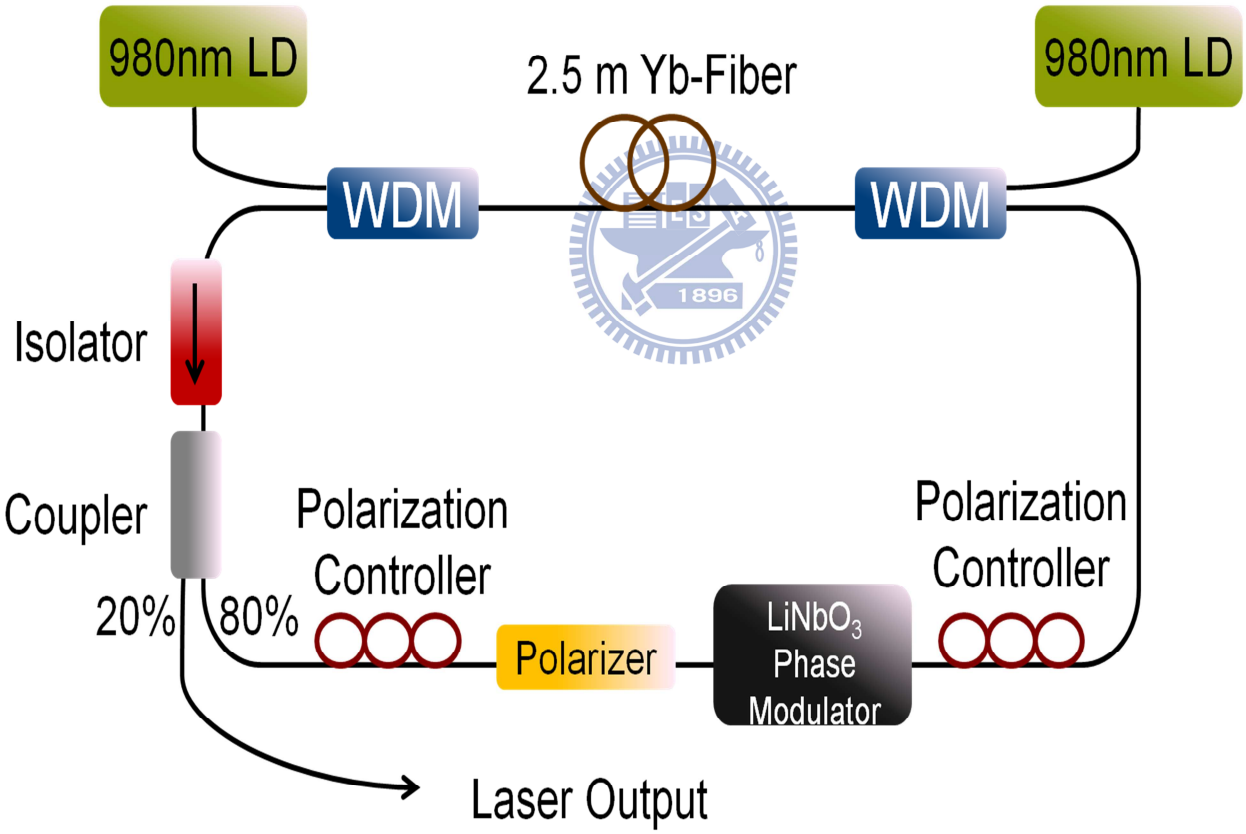

Fig. 3.1 The experimental setup.

Two laser diodes with the 976 nm central wavelength is used to pump the 2.5 m long Yb-doped fiber （Nufern SM-YSF-LO） , which acts as the laser gain medium, through a wavelength-division multiplexing（WDM）coupler. The output coupler is located behind the Yb-fiber in order to getting the greatest output power. The coupling ratio is 20/80 so that the coupler will couple 20% power of laser cavity as laser output. An isolator in the ring cavity is to ensure the pulses propagate in only one direction. The $LiNbO_3$ phase modulator in the ring cavity is used to achieve actively harmonic mode-locking by EO effect. The average cavity length is estimated to be 23.1 m. The devices that have been used in the fiber ring cavity are listed in table 3.1.

Device	Specification
Single Mode Fiber @ 1060nm (HI1060)	Attenuation (dB/km) : 2.1 @ 980 nm ,1.5 @ 1060 nm Dispersion (ps/nm/km) : -53 @ 980 nm ,-38 @ 1060 nm
Ytterbium-Doped Fiber (Nufern SM-YSF-LO)	Core absorption(dB/km) : 80@ 980 nm Dispersion (ps/nm/km) : -37 @ 1060 nm
$LiNbO_3$ phase modulator	Insertion loss(dB) : 1.7 RF V_π(@ 1 GHz, Volts) : 3.0 Polarization crosstalk(dB) : 18
Polarization Independent Isolator	Isolation(dB): 40.0 Insertion loss(dB): 1.51
WDM Coupler(980/1064 nm)	Isolation(dB): 26.0 @ 980 nm ,23.3 @ 1060 nm Insertion loss(dB): 0.3 @ 980 nm ,0.24 @ 1060 nm
Coupler	Splitting ratio : 20/80 @ 1060 nm
Polarizer	Extinction ratio (dB) : 28 Isolation(dB) : 0.45
980nm Pump Laser	Maximum output power(mW): 450

Table 3.1 The devices in the fiber ring cavity

3.2 Harmonic mode-locking results

From section 2.2, we know that if the modulation signal is equal to integer multiple of the fundamental frequency, pulse trains with a higher repetition rate than the fundamental frequency can be generated by the laser system. Base on the experimental setup shown in the section 3.1, we can drive modulation frequency in the laser cavity synchronously so that one can achieve harmonic mode-locking.

The fiber type in the fiber laser cavity can be divided into two parts : the single mode fiber （HI 1060） length is about 20.6 meters and the ytterbium-doped fiber length is about 2.5 meters. The total length is 23.1 meters for this cavity. So the fundamental frequency of the laser is estimated to be $f_0 = c/nL = 8.67$ MHz. The net cavity dispersion is around 0.7113 ps^2. The bi-directional pumping is utilized in the setup and about 275mW of 976 nm pumping power is used in the laser. A synthesizer is used to generate the RF driving signal which is then amplified to 30dBm. The electrical driving signal for the phase-modulator is provided by a microwave signal generator (R&S SMR40) and amplified by a power amplifier (Agilent 83017A).

First, we can drive the phase modulator at the modulation frequency 1.0005867 GHz, and the laser was perfectly mode-locked with the several times of repetition rate around 1GHz. In this case, the laser is driven by bi-directional pumping and the pumping power is around 175 mW. Then we can adjust the polarization controller to achieve mode-locking.

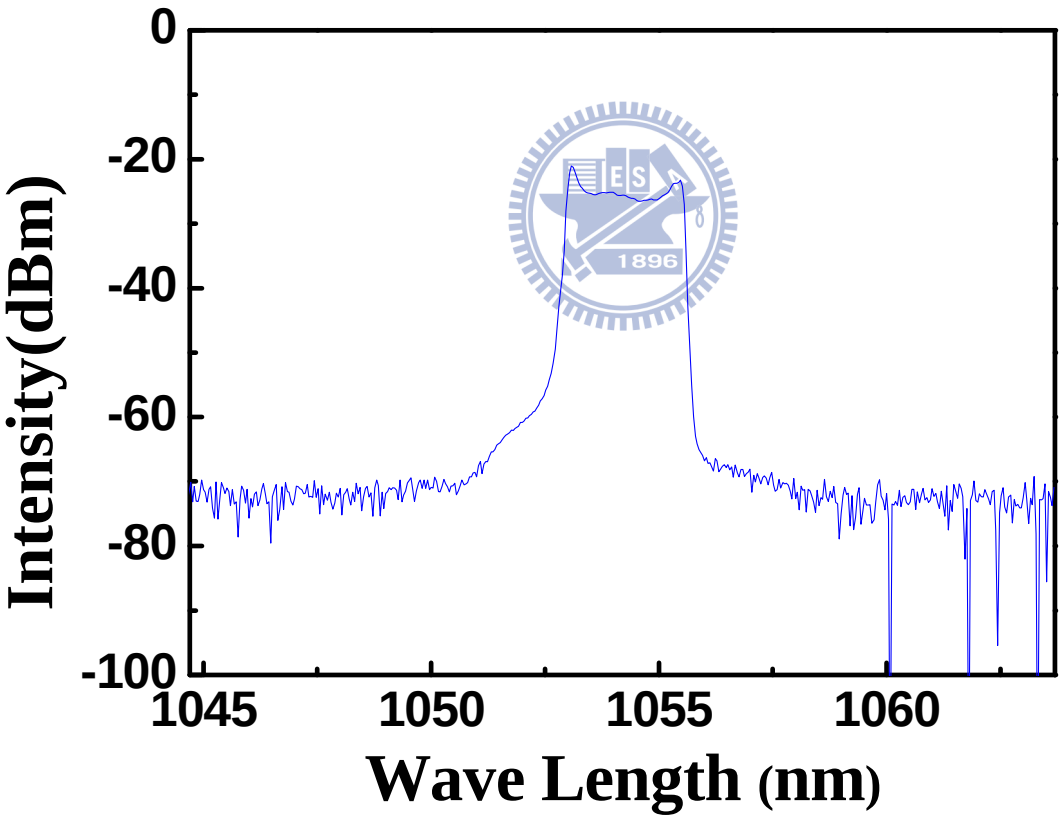

Fig. 3.2 The optical spectrum of the laser output

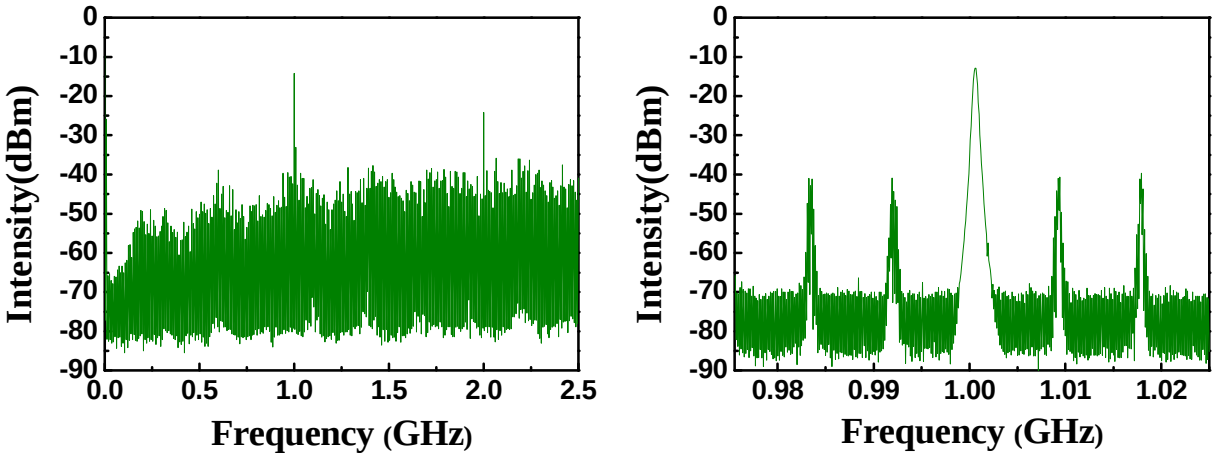

Fig. 3.3&3.4 The RF spectrum with span = 2.5 GHz and 50 MHz, resolution bandwidth = 300 kHz and3 kHz

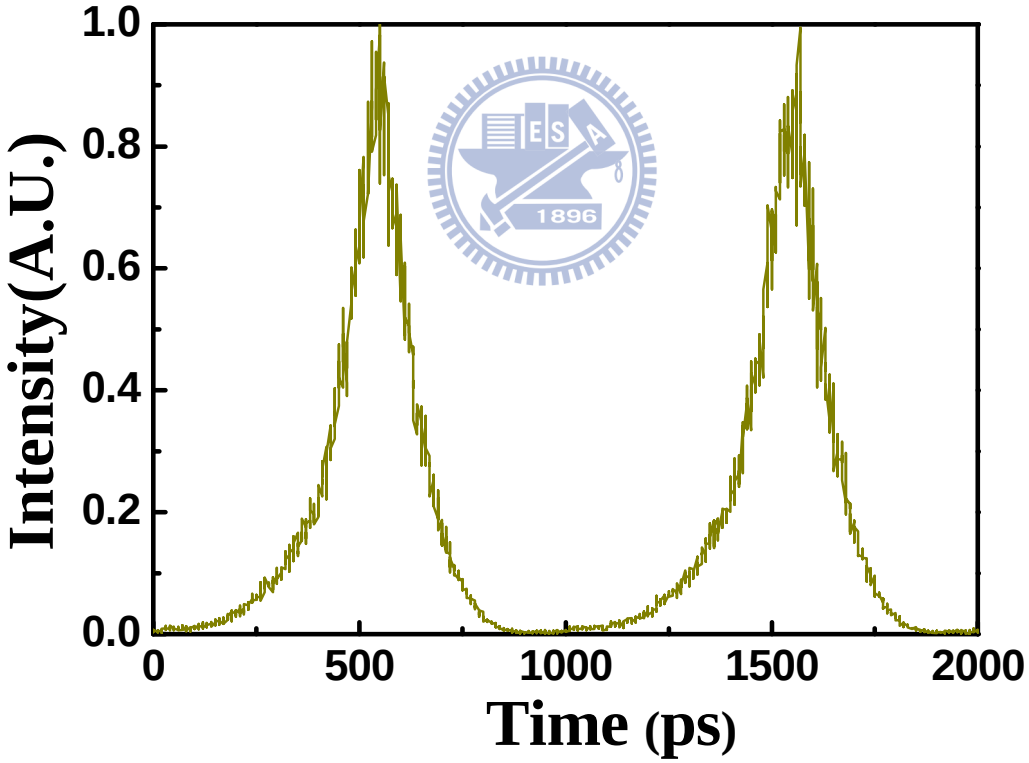

Fig. 3.5 1 GHz pulse trains by the 20 GHz fast sampling oscilloscope

For this case, the bandwidth of the optical spectrum is around 2.52 nm（Fig.

3.2）. In the RF spectrum, the noise floor is high. It could be caused by the super-mode noises since the super-mode suppression ratio is around 20 dB as illustrated in Fig. 3.4. This large super-mode noise may be due to the gain competition caused by unwanted harmonic modes.

Moreover, we also can drive the laser around 5 GHz, and the precise pulse repetition rate is 5.028742 GHz. In this case, the laser is also driven by bi-directional pumping and the pumping power is around 175 mW. One can observe that the bandwidth of optical spectrum is 1.636 nm.

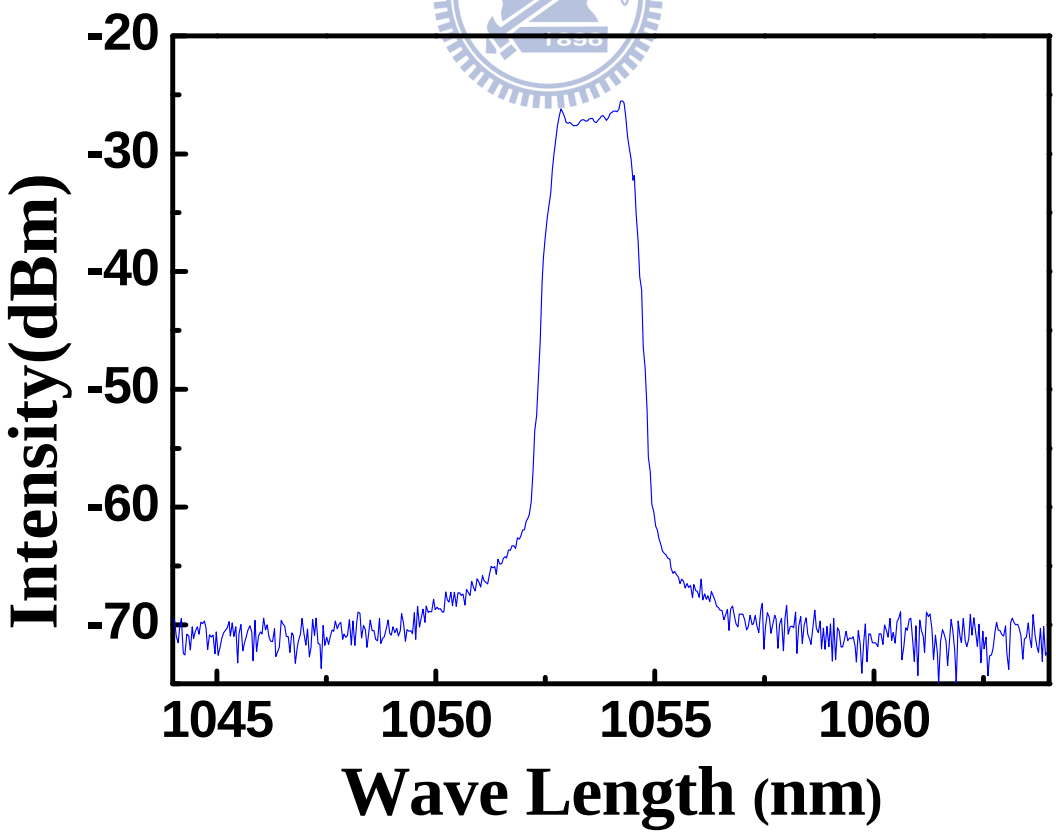

Fig. 3.6 The optical spectrum of the laser output

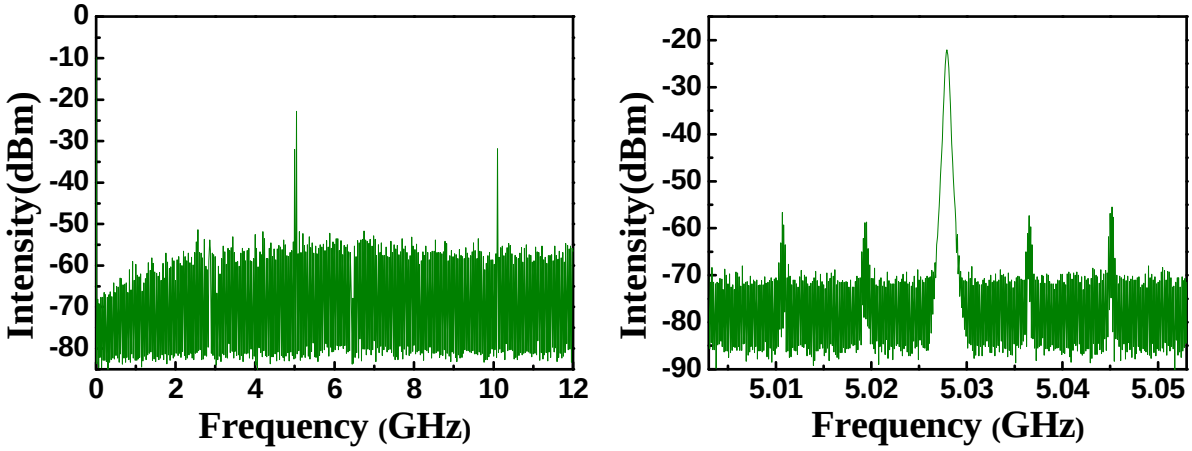

Fig. 3.7&3.8 The RF spectrum with span = 12 GHz and 50 MHz, resolution bandwidth = 300 kHz and 3 kHz

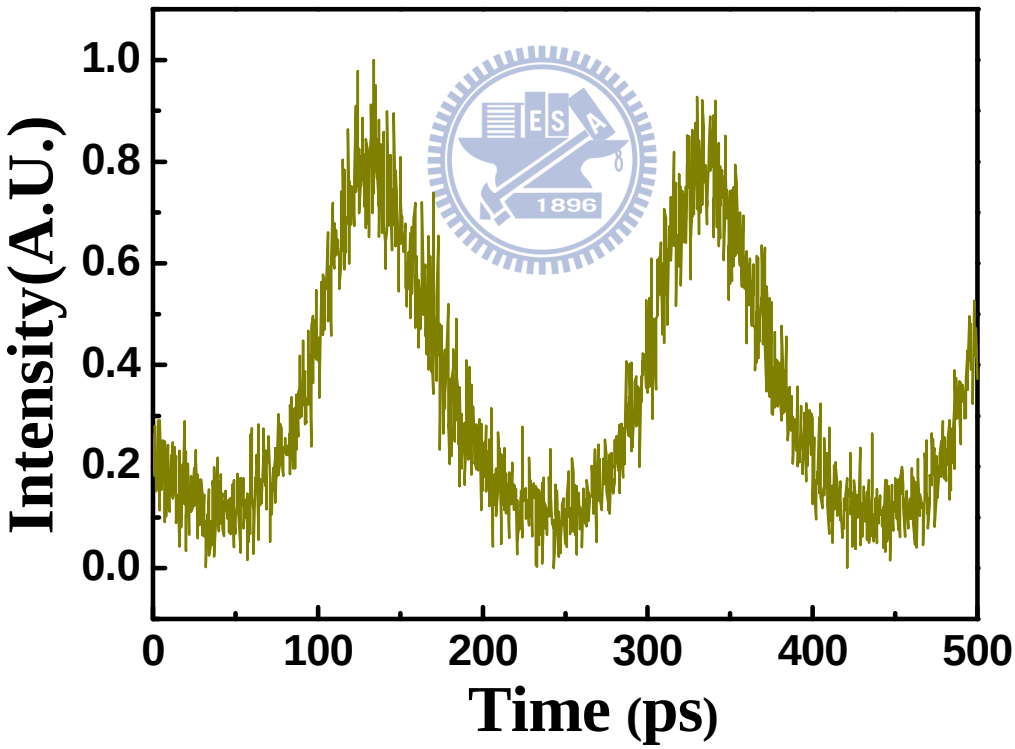

Fig. 3.9 5 GHz pulse trains by the 20 GHz fast sampling oscilloscope

For this case, the bandwidth of optical spectrum is around 1.636 nm（Fig.

3.5）. In the RF spectrum, the noise floor is lower than previous case. The super-mode suppression ratio is around 30 dB

Moreover, we drive the phase modulator around 10 GHz, and the precise pulse repetition rate is 10.005937 GHz. In this case, the laser is also driven by bi-directional pumping and the pumping power is around 175 mW. We then adjust the polarization controller to let the laser achieve the mode-locking state.

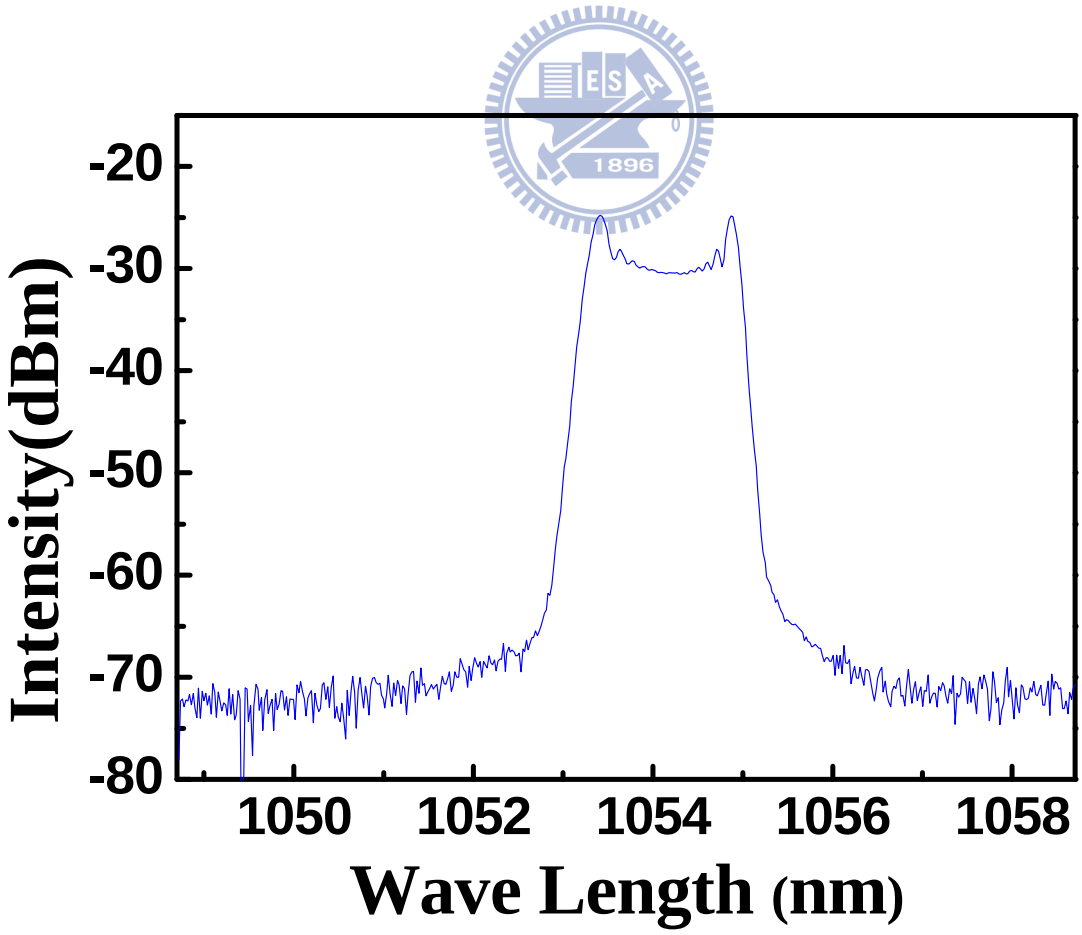

Fig. 3.10 The optical spectrum of the laser output

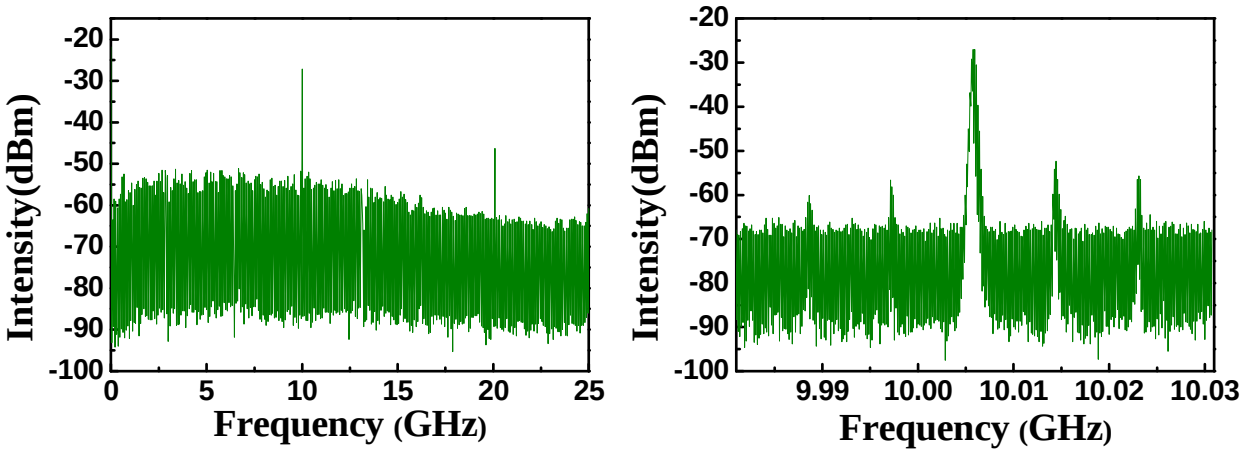

Fig. 3.11&3.12 The RF spectrum with span = 25 GHz and 50 MHz, resolution bandwidth = 300 kHz and 3 kHz

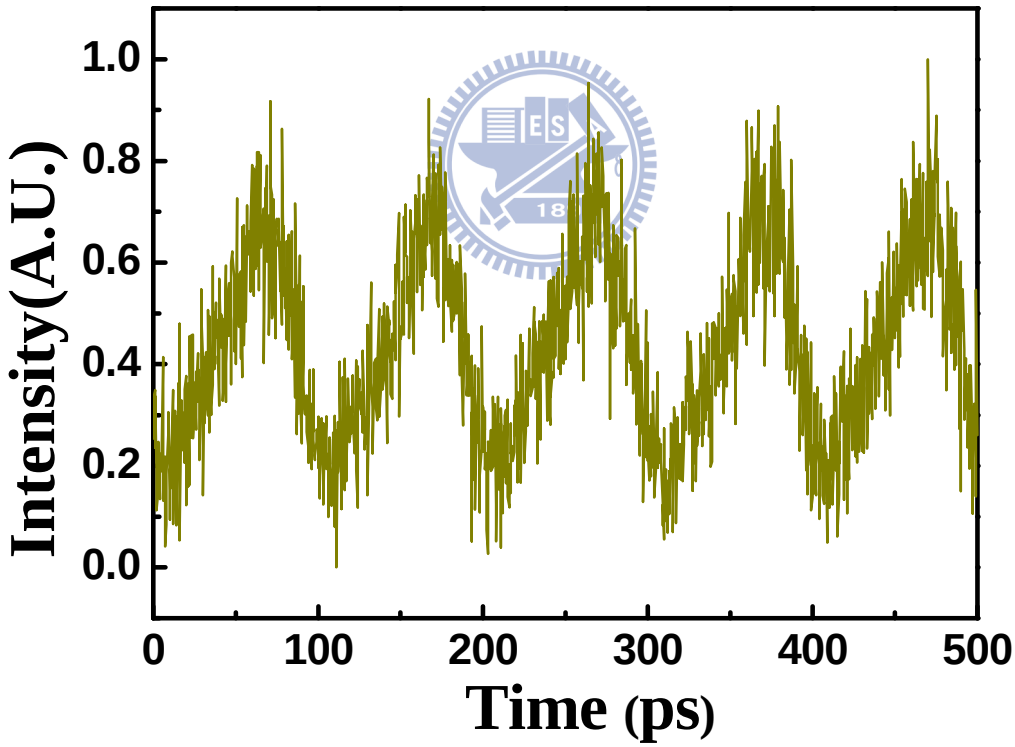

Fig. 3.13 10 GHz pulse trains by the 20 GHz fast sampling oscilloscope

For this case, the bandwidth of optical spectrum is around 1.677 nm（Fig.

3.10）. In the RF spectrum, the noise floor is lower than previous case. The super-mode suppression ratio is still around 30 dB

In summary, although the repetition rate can increase to the order of 10 GHz, the super-mode noise in the synchronous harmonic mode-locked laser is pretty large due to the gain competition between many super-modes in the ytterbium gain spectrum. Super-mode noises may cause un-equalization intensity of pulse train in time domain, and generally it is hard to reduce them for harmonic mode-locking. In these three harmonic mode-locked cases, we can observe the pulse train signal on the 20 GHz fast sampling oscilloscope. However, we can not see the signals on the autocorrelator. This may be because that the pulsewidth of these cases are too large to detect from autocorrelator due to too low peak power. For most of applications in the fields of optical communication or bio-photonics, un-equalized intensity and large pulsewidth is not a good characteristic. So in next section, we will demonstrate of an asynchronous harmonic mode-locked ytterbium laser with much smaller super-mode noises.

3.3 Asynchronous harmonic mode-locking results

In section 3.2, we have demonstrated that the harmonic mode-locking can be achieved in this experimental setup. However, at the harmonic mode-locking operation state, the super-mode suppression ratio is relatively high. In this section, the experimental results of asynchronous harmonic mode-locking will be presented.

Form section 2.3, we can predict that the super-mode noise can be suppressed well at the asynchronous harmonic mode-locking operation state. Compared with harmonic mode-locking, asynchronous harmonic mode-locking has an additional deviation frequency between the modulation frequency and cavity frequency. The optical pulses do not always pass through at the peaks of the modulation signal. The linear noises will follow the asynchronous phase modulation signal and shift the central frequency. In the way, the super-mode noises can be suppressed successfully. The frequency will shift out of the filter bandwidth. Because of the limitation of optical filter and gain bandwidth, linear noises will experience huge loss and will be suppressed in the laser cavity. Nevertheless, nonlinear optical pulses will stay in the laser cavity stably.

So we will generate pulse trains by asynchronous harmonic mode-locking and observe whether the super-mode suppression ratio of the laser is increased or not in this section. In our prediction, the asynchronous harmonic mode-locking should suppress the super-mode more and the noises will be smaller than harmonic mode-locking.

As first step, we asynchronously drive the EO modulator around 5.002753 GHz. By detuning the modulation frequency with a small amount of kHz and adjusting the polarization controllers, we can achieve a stable mode-locked state. In this case, the laser is only driven by the forward pump and the pumping power is 175 mW.

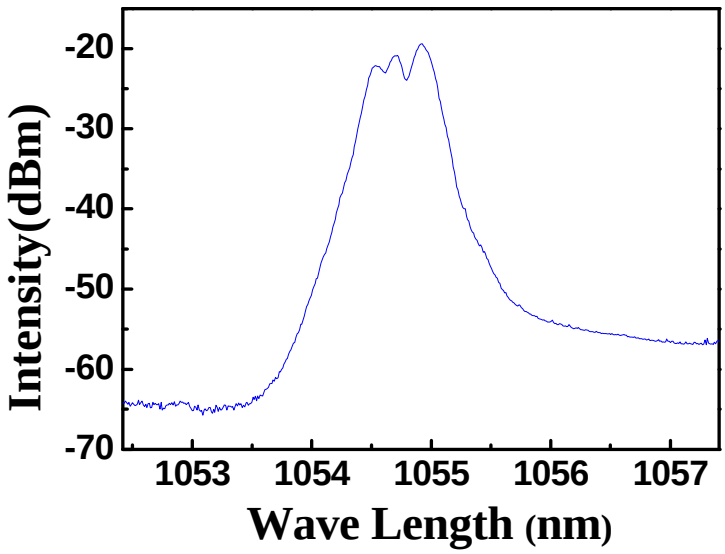

Fig. 3.14 The optical spectrum of the laser output

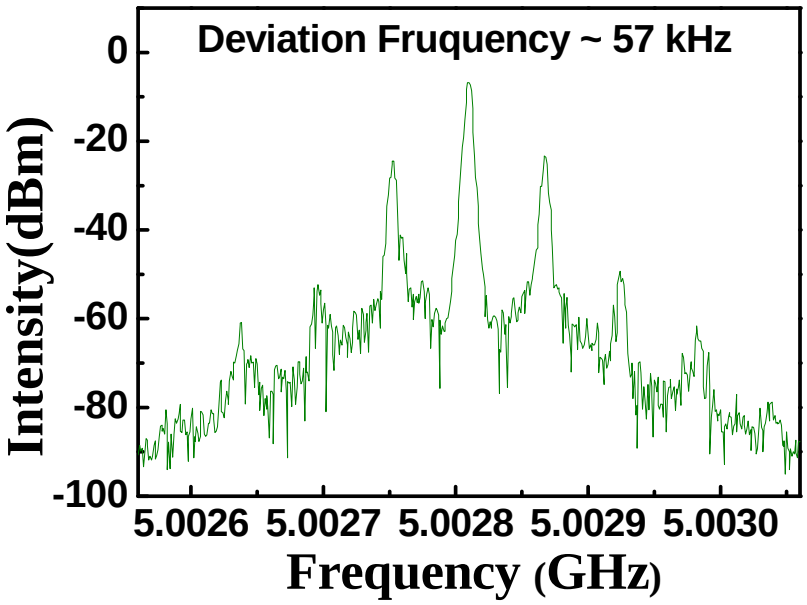

Fig. 3.15 The RF spectrum with span = 500 KHz, resolution bandwidth = 3 kHz

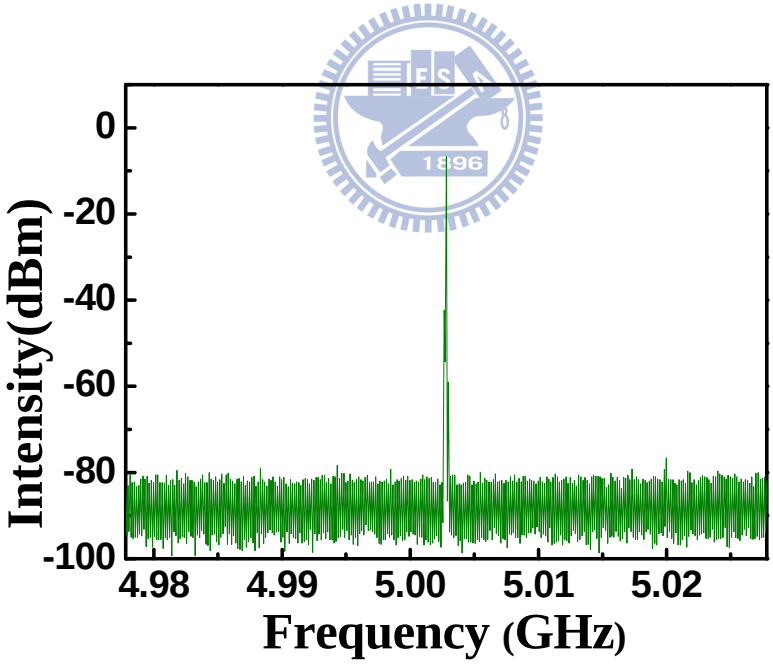

Fig. 3.16 The RF spectrum with span = 50 MHz, resolution bandwidth = 10 kHz

In this case, the laser is operated at the asynchronous harmonic mode-locking state due to the asynchronously driving of the phase modulator.

From Fig 3.15, one can see the RF spectrum of the asynchronous mode-locked laser with the deviation frequency around 57 kHz. Therefore, from Fig 3.16, we can obviously observe that the super-mode noises can be suppressed as our prediction, and the super-mode suppression ratio achieved is around 75 dB.

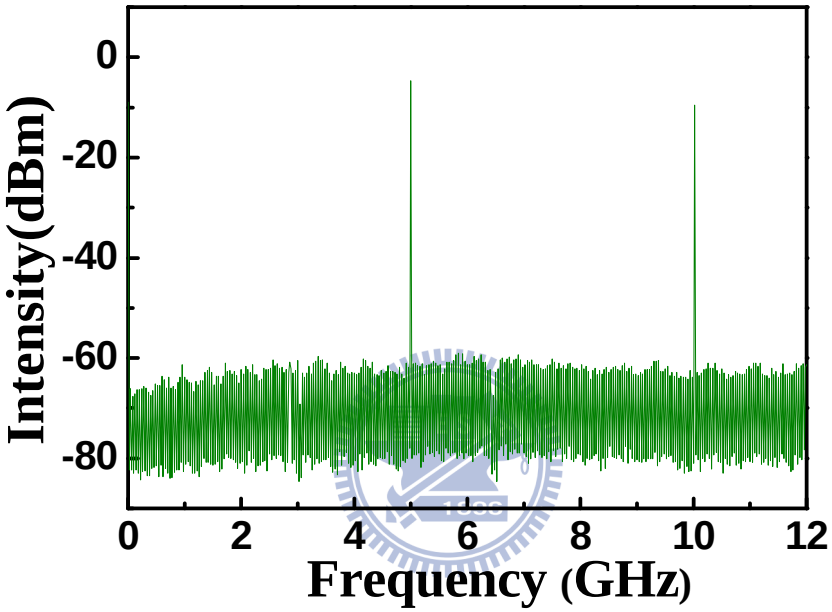

Fig. 3.17 The RF spectrum with span = 12 GHz, resolution bandwidth = 300 kHz

We can obviously observe that the super-mode suppression ratio does increase very much than the previous 5 GHz synchronous harmonic mode-locking cases. Fig 3.17 is the RF spectrum with span from DC to 12 GHz, and the super-mode noise is pretty good. The super-mode suppression ratio is around 60 dB as before.

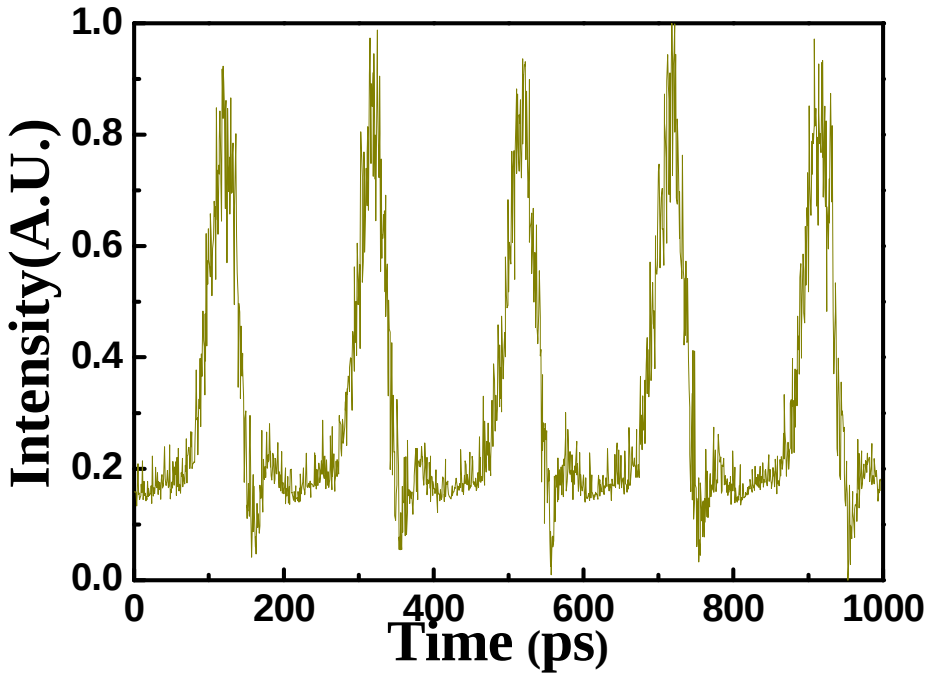

Fig. 3.18 5 GHz pulse trains by the 20 GHz fast sampling oscilloscope

Fig. 3.18 is the 5.0028308 GHz pulse trains detected by the 20 GHz fast sampling oscilloscope in the time domain. The pulsewidth show on the machine is about 50 ps, which is the resolution limit of the fast sampling oscilloscope we use. From the resolution limit of the oscilloscope time tracing, we can know that the real pulsewidth should be shorter than 50 ps in the 5 GHz asynchronous harmonic mode-locked case. The real pulsewidth is determined by the autocorrelator.

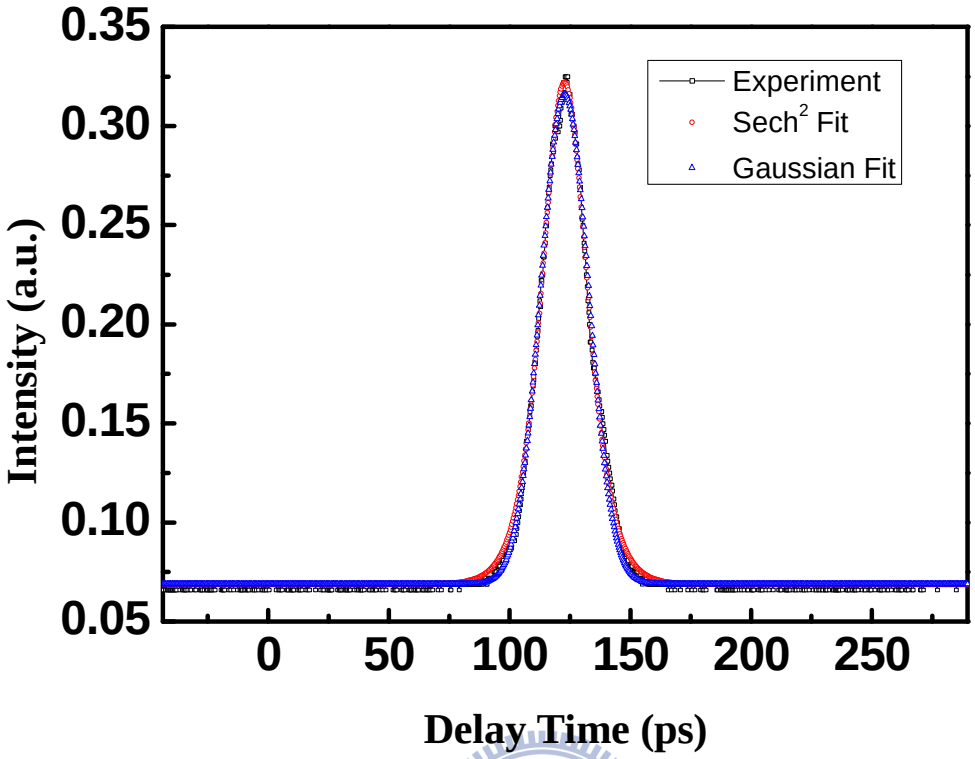

Fig. 19 SHG intensity autocorrelation trace （solid curve） of 5 GHz pulse train and the fitting curve （open circles and open triangles） of the laser output, assuming $Sech^2$ and Gaussian pulse shape.

The solid curve in Fig. 19 is the fitting of the SHG intensity autocorrelation trace with the assumption of $Sech^2$ and Gaussian pulse shape, and the FWHM of the SHG intensity autocorrelation trace is 22.2627 ps. If the autocorrelation trace is fit with $Sech^2$ and Gaussian profiles respectively, the inferred pulse durations are 14.4563 ps and 16.4499 ps.

We then drive the phase modulator at 10.005897 GHz. 10 GHz is the bandwidth limit of our modulator, so we can not operate at higher frequencies unless we change another modulator. In this case, the laser is also driven by bi-directional pumping and the pumping power is around 175 mW. By adjusting the polarizers, we not only can achieve the mode-locked state but also can find an operating point that has less super-mode noises. Moreover, Fig. 3.20 shows that the 3dB bandwidth of the optical spectrum is 1.15 nm.

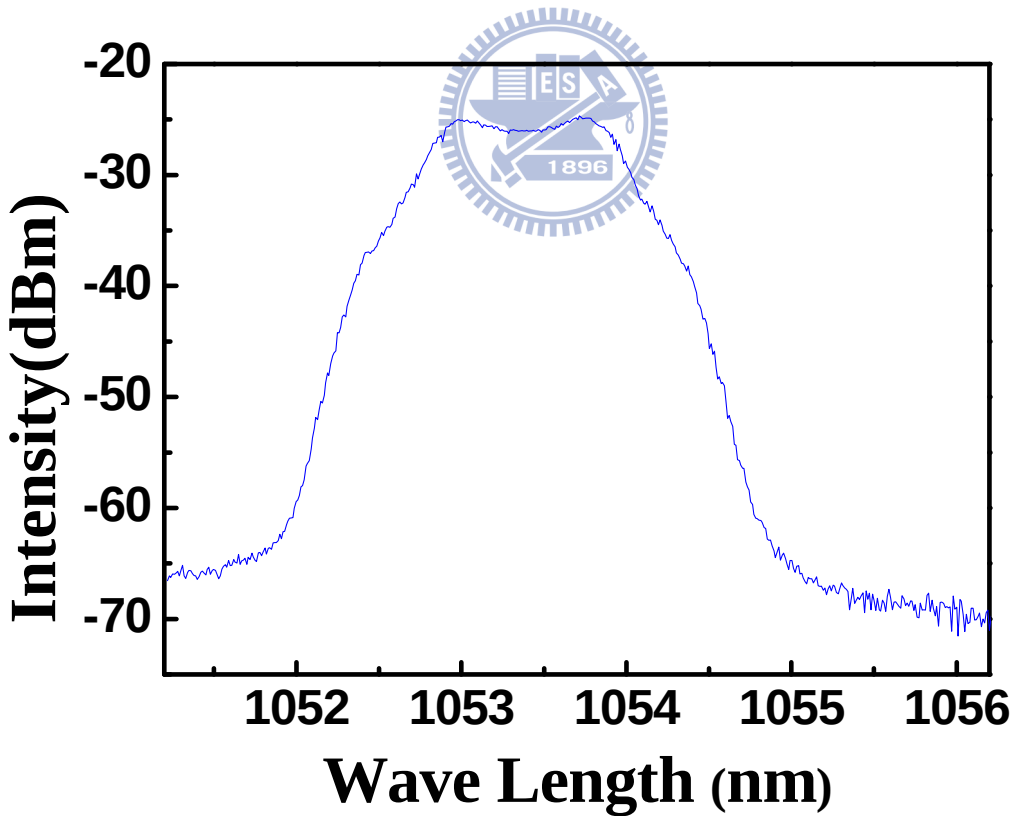

Fig. 3.20 The optical spectrum of the laser output

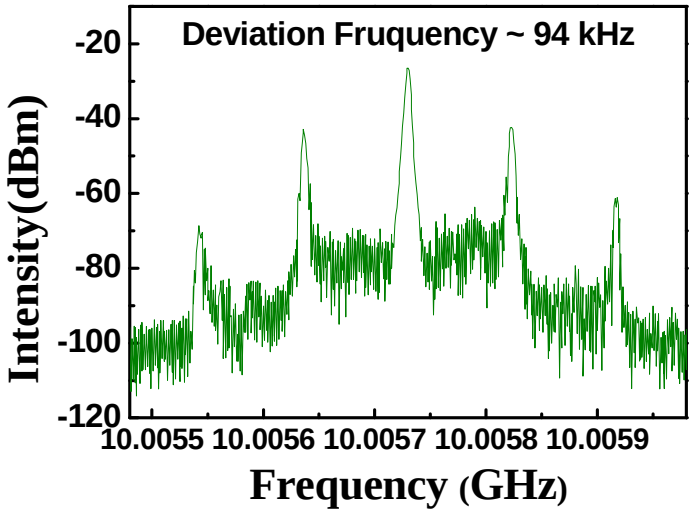

Fig. 3.21 The RF spectrum with span = 500 KHz, resolution bandwidth = 3 kHz

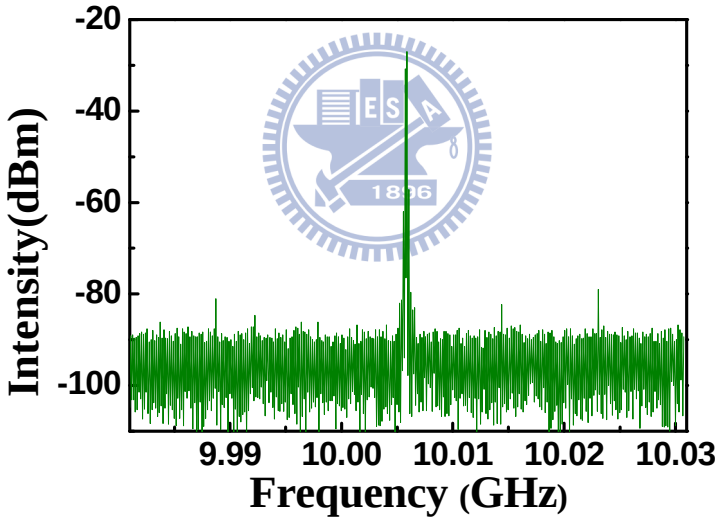

Fig. 3.22 The RF spectrum with span = 50 MHz, resolution bandwidth = 10 kHz

For the illustrating case presented in Fig. 3.22, from the RF spectrum of the output pulse train. It can be seen that the super-mode suppression ratio in the RF spectrum is as high as 53dB. It is still much better than the case operating at the

synchronous mode-locked state. The 1166th harmonic cavity frequency is 10.005729 GHz, and the modulation frequency is 10.005823 GHz. The detuning between the modulation frequency and the cavity harmonic frequency can be clearly observed through the beating signals, with the spectral spacing equal to the frequency deviation of 94 kHz.

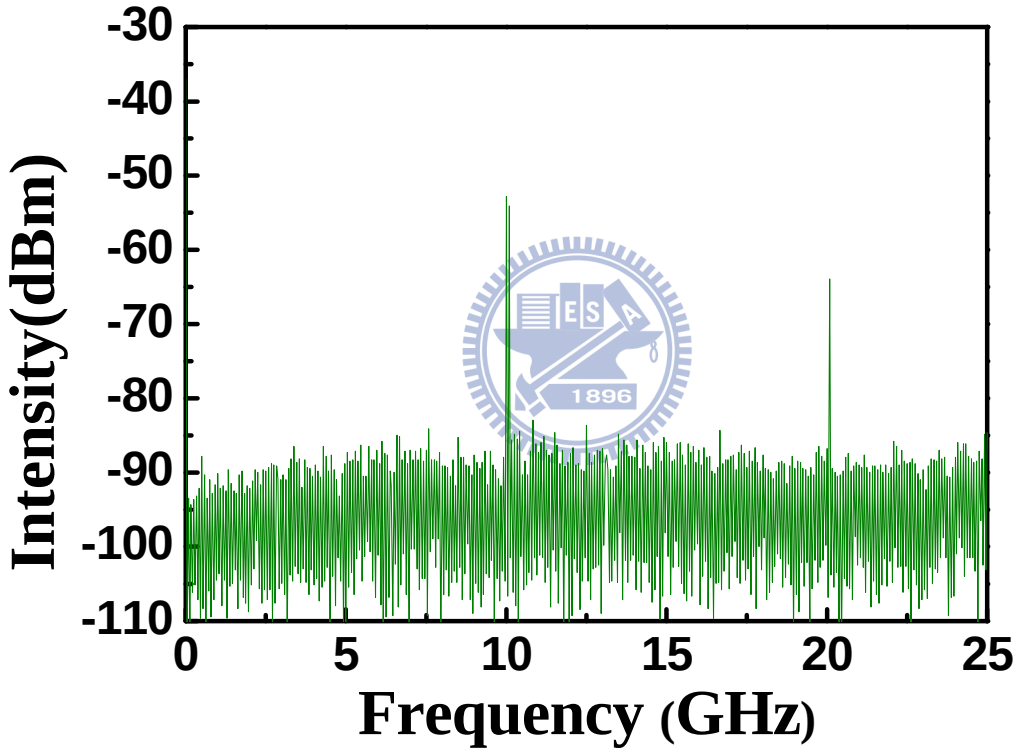

Fig. 3.23 The RF spectrum with span = 25 GHz, resolution bandwidth = 300 kHz

Fig. 3.23 shows the Rf frequency components from DC to 25GHz. We can observe that there are two peaks caused by the repetition rate of the pulse train.

The noise floor of this asynchronous state is lower than all previous synchronous cases, and it is lower about 20 dB if compared with the 10 GHz synchronous cases.

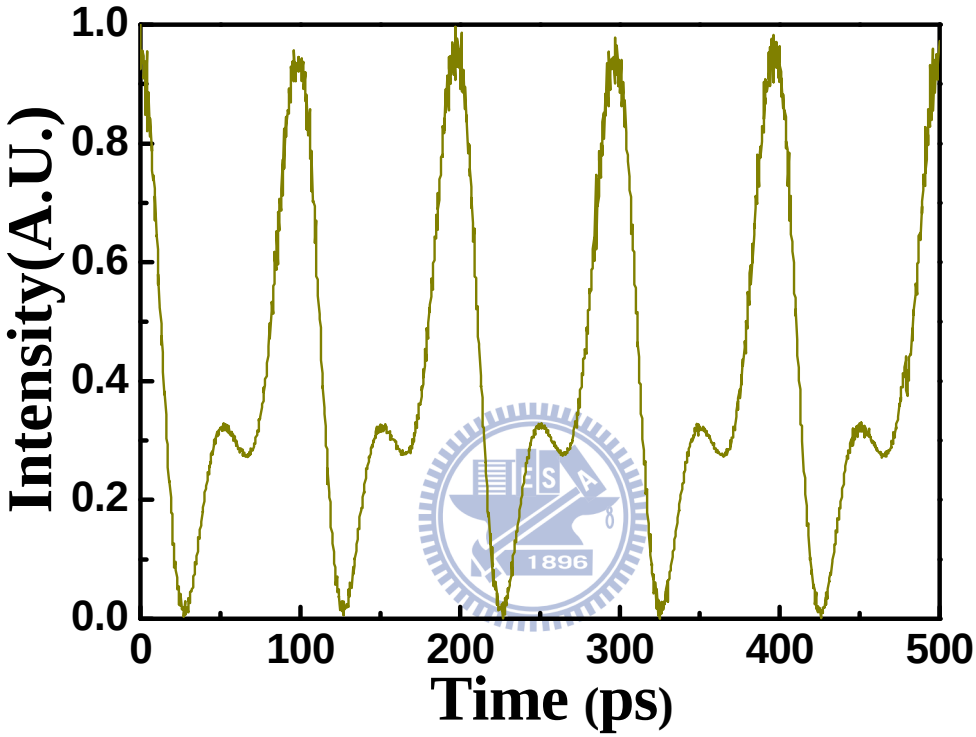

Fig. 3.24 10 GHz pulse trains by the 20 GHz fast sampling oscilloscope

Fig. 3.24 is the 10.005729 GHz pulse trains detected by the 20 GHz fast sampling oscilloscope in time domain. The pulsewidth show on the machine is about 20 ps, which is below the resolution limit of fast sampling oscilloscope. The real pulsewidth is determined by the autocorrelator.

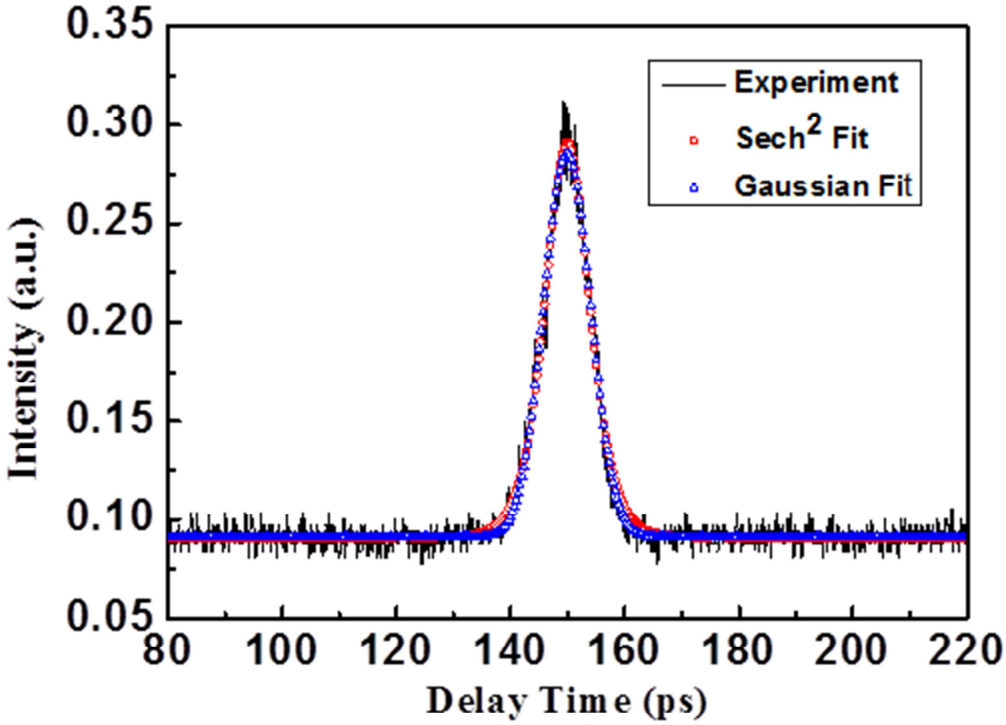

Fig. 3.25 SHG intensity autocorrelation trace（solid curve）of 10 GHz pulse train and the fitting curve（open circles and open triangles）of the laser output, assuming $Sech^2$ and Gaussian pulse shape.

The solid curve in Fig. 25 is the fitting of the SHG intensity autocorrelation trace with the assumption of $Sech^2$ and Gaussian pulse shape, and the FWHM of the SHG intensity autocorrelation trace is 9.1405 ps. If the autocorrelation trace is fit with $Sech^2$ and Gaussian profiles respectively, the inferred pulse durations are 5.9354 ps and 6.8292 ps.

As a summary of the results, the super-mode suppression ratio is around 20 dB for synchronous harmonic mode-locking, and 50 dB for asynchronous harmonic mode-locking. Therefore, if the laser is operating at the asynchronous harmonic mode-locked state, we should be able to get much higher super-mode suppression ratios than operating at the synchronous harmonic mode-locked state from previous sections. Moreover, the noise floor of the asynchronous harmonic mode-locked case is lower than the synchronous harmonic mode-locking too. And the output power of asynchronous harmonic mode-locking is around 20mW. Furthermore, in the time domain, the pulsewidth of 10 GHz synchronous harmonic mode-locked state can be short as 5.9354 ps ($Sech^2$ Fit) and 6.8292 ps (Gaussian Fit). However, we observe a disadvantage in which the optical bandwidth of the asynchronous harmonic mode-locked state is smaller than the synchronous harmonic mode-locked state. It means that the transform-limited pulsewidth will be larger in this experimental condition. However, the pulsewidth of the synchronous harmonic mode-locked state is too large to be detected from autocorrelator while the asynchronous harmonic mode-locked case can be detected. It may be because that the pulse in the normal dispersion region has larger chirp as well as large pulsewidth.

Reference

[3.1] G. Lin, M. Wu, and Y. Chang, “Suppression of phase and supermode noise in a harmonic mode-locked erbium-doped fiber laser with a semiconductor-optical-amplifier-based high-pass filter”, Opt. Lett., 30, 1834–1836 (2005).

[3.2] F. Quinlan, S. Gee, S. Ozharar, and P. J. Delfyett, “Ultralow-jitter and -amplitude-noise semiconductor-based actively mode-locked laser”, Opt. Lett., 31, 2870–2872 (2006).

[3.3] J. Chen, J. W. Sickler, E. P. Ippen, and . X. Kärtner, “ High repetition rate, low jitter, low intensity noise, fundamentally mode-locked 167 fs soliton Er-fiber laser”, Opt. Lett., 32, 1566–1568 (2007).

[3.4] M. Nakazawa, K. Tamura and E. Yoshida, “Supermode noise suppression in a harmonically modelocked fibre laser by selfphase modulation and spectral filtering”, Electron. Lett., 32,461-463 (1996).

[3.5] M. Nakazawa, and E. Yoshida, “SA 40-GHz 850-fs Regeneratively FM Mode-Locked Polarization-Maintaining Erbium Fiber Ring Laser”, IEEE Photon. Technol. Lett., 12, 1613-1615 (2000).

Chapter 4

Conclusions

4.1 Summary of achievements

In summary, we have for the first time successfully demonstrated an asynchronous harmonic mode-locked ytterbium doped fiber laser with 10 GHz EO phase modulation. The asynchronous harmonic mode-locked ytterbium doped fiber laser can stably work in the normal dispersion region. We find that the asynchronous mode-locking mechanism can not only exist in the anomalous net dispersion regionas in the previously studied asynchronous harmonic mode-locked erbium doped fiber soliton lasers but also can work in thenormal dispersion regime such as ytterbium doped fiber laser.

Secondly, from the experimental results, we can observe 10 GHz stable ps-order pulse trains with good super-mode suppression ratio （60 dB）. The laser is operated about 1050　nm with a deviation frequency about 94 KHz and output power about 20 mW.

Thirdly, the optical bandwidth in asynchronous harmonic mode-locking is

smaller than at the synchronous harmonic mode-locked operation state. The result reveals the effective nonlinearity may be smaller in the present asynchronous harmonic mode-locking case. The real effect will be found by further experiment.

Finally, theoretical simulation based on the master equation model has also been carried out to prove the existence of asynchronous mode-locked steady state solution. These results indicate the existence of a totally different operation regime of asynchronous harmonic mode-locking and may be useful for constructing higher repetition rate mode-locked ytterbium doped fiber lasers.

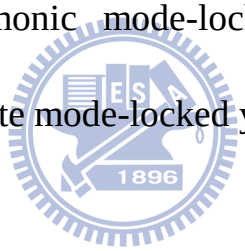

4.2 Future work

This thesis has successfully demonstrated the high repetition pulse trains with center wavelength about 1050 nm. However, if we change the pumping power condition into higher power, there are CW components built up. These unwanted components will have bad effects for the mode-locking. Therefore, in the future work, we may be able to use the band-pass filter to suppress the CW components when the laser is operated in the high pumping powers. Then, we can obtain higher output powers. The laser is also supposed to operate at much higher repetition rates with another modulator that can be operated at higher frequencies.

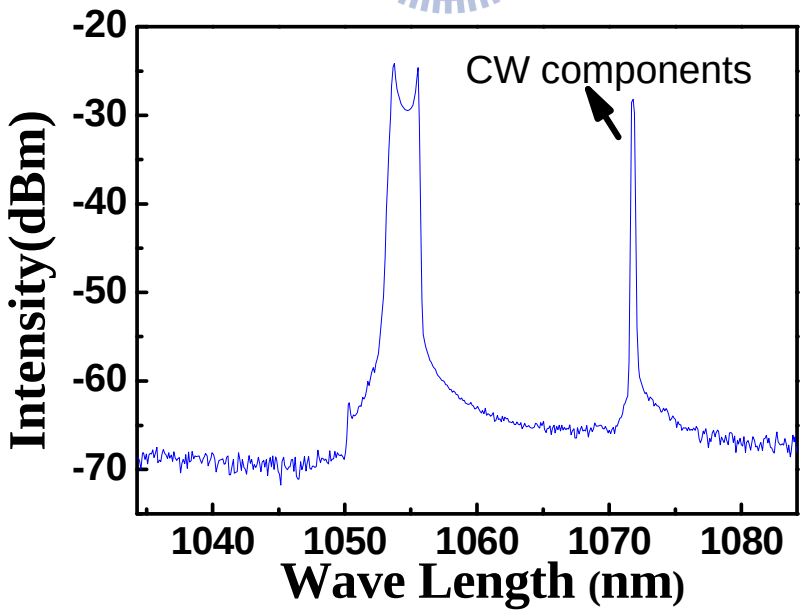

Fig. 4.1 The CW components when the laser is operated in the high pumping powers.